



Shelf-edge glaciation offshore of northeast Greenland during the last glacial maximum and timing of initial ice-sheet retreat

Colm Ó Cofaigh^{a,*}, Jeremy M. Lloyd^a, S. Louise Callard^b, Catalina Gebhardt^c, Katharina T. Streuff^d, Boris Dorschel^c, James A. Smith^e, Timothy P. Lane^f, Stewart S.R. Jamieson^a, Torsten Kanzow^c, David H. Roberts^a

^a Department of Geography, Durham University, UK

^b Department of Geography, University of Newcastle, Newcastle, UK

^c Alfred Wegener Institute Helmholtz Centre for Polar and Marine Research, Bremerhaven, Germany

^d Faculty of Geosciences and MARUM - Center for Marine Environmental Sciences, University of Bremen, Bremen, Germany

^e British Antarctic Survey, High Cross, Madingley Road, Cambridge, CB3 0ET, UK

^f Department of Geoscience, Aarhus University, Denmark

ARTICLE INFO

Handling editor: A. Voelker

Keywords:

Greenland ice sheet
Last glacial maximum
Ice sheet extent
Grounding-zone wedges
Glacimarine
Deglaciation
Ice-sheet retreat

ABSTRACT

This paper presents new marine geophysical data and radiocarbon dated sediment cores to reconstruct the maximum extent of the Northeast Greenland Ice Stream (NEGIS) during the last glaciation and the timing of its initial retreat from the continental shelf. The NEGIS is the largest ice stream to drain the Greenland Ice Sheet (GrIS) today, and holds a sea-level equivalent of 1.1–1.4 m. It has undergone recent retreat but the longer-term history of NEGIS on the adjoining continental shelf is still relatively poorly constrained. Two cross-shelf bathymetric troughs, Westwind and Norske troughs, acted as pathways for offshore-flowing ice during the last glaciation but little is known about the acoustic stratigraphy, sedimentology and chronology of ice sheet retreat in the outer shelf sections of both troughs. Multibeam swath bathymetry and acoustic data from both troughs show flow parallel and flow transverse glacial landforms in the outer shelf sections of both troughs. Mega-scale glacial lineations in Westwind Trough record former streaming flow towards the shelf-edge. Grounding-zone wedges record episodic stabilisation during retreat from the shelf-edge. Sediment cores recovered subglacial tills and grounding-zone proximal sediments overlain by glacimarine sediments. The slope beyond Norske Trough is characterised by glacial debris flows typical of submarine slopes offshore of shelf-edge terminating palaeo-ice streams. Radiocarbon dates indicate that initial retreat of the ancestral NEGIS from the northeast Greenland shelf-edge was underway by 21.5–21.6 cal ka BP in Norske Trough and $c. \geq 19.0$ cal ka BP in Westwind Trough. Retreat rates across the outer shelf were slow at 19–23 m a⁻¹ but increased across the inner shelf. Our data provides the first direct chronological support for a shelf-edge terminating GrIS offshore of northeast Greenland during the last glacial maximum and demonstrates this sector of the GrIS underwent relatively early retreat from the shelf-edge.

1. Introduction

The Greenland Ice Sheet (GrIS) is the only extant ice sheet in the northern hemisphere today and contains a sea level equivalent of c. 7 m (Aschwanden et al., 2019). Over the last few decades many sectors of the ice sheet have experienced significant mass loss and rapid changes to flow dynamics in response to atmospheric and oceanic warming (e.g., Rignot and Kanagaratnam, 2006; Mouginit et al., 2015; Rignot et al.,

2016; Khan et al., 2014, 2022; Schaffer et al., 2020; An et al., 2021; Wekerle et al., 2024). One such sector is northeast Greenland where the Northeast Greenland Ice Stream (NEGIS), the largest ice stream of the contemporary GrIS, drains about 16 % of the ice sheet and contains a sea level equivalent of 1.1–1.4 m (Mouginit et al., 2015). The NEGIS extends for about 700 km from the present coastline inland to the Greenland summit. It terminates in three outlets: 79N Glacier (also known as Nioghalvfjærdsfjorden Glacier), Zachariae Isstrøm (ZI) and

* Corresponding author.

E-mail address: colm.ocofaigh@durham.ac.uk (C. Ó Cofaigh).

<https://doi.org/10.1016/j.quascirev.2025.109326>

Received 19 August 2024; Received in revised form 14 March 2025; Accepted 21 March 2025

Available online 19 April 2025

0277-3791/© 2025 The Authors. Published by Elsevier Ltd. This is an open access article under the CC BY license (<http://creativecommons.org/licenses/by/4.0/>).

Storstrømmen. 79N Glacier is buttressed by a floating ice tongue which is the largest extant ice shelf in Greenland today. Recent observations show that it has thinned by c. 30 % between 1999 and 2014, with submarine melt proposed as a major driver of this thinning (Mayer et al., 2018; Lindeman et al., 2020; Wekerle et al., 2024). The floating tongue of ZI disintegrated completely from 2005 to 2015 (Mouginot et al., 2015).

Critical to understanding the longer-term trajectory of changes to the contemporary GrIS is an understanding of the ice sheet history for the period prior to instrumental records. Despite significant advances in reconstructing this history from both terrestrial (e.g., Bennike and Björck, 2002; Briner et al., 2010; Young et al., 2011; Roberts et al., 2013, 2024; Lane et al., 2015, 2023; Larsen et al., 2018) and marine archives (e.g., Ó Cofaigh et al., 2004, 2013a; Hogan et al., 2016; Slabon et al., 2016; Newton et al., 2017; Skov et al., 2020; Hansen et al., 2022; Lloyd et al., 2023; Callard et al. *subm.*) there remain major gaps in our understanding of GrIS history during the last glacial maximum (LGM) when the ice sheet expanded onto the continental shelf around Greenland.

Early terrestrial work on GrIS history in northeast Greenland proposed that the ice sheet did not extend beyond the inner shelf at the LGM (see Funder et al., 2011). Subsequent marine geophysical investigations from the middle continental shelf, however, identified a number of flow parallel and flow transverse ice sheet landforms in the cross-shelf bathymetric troughs. Initial observations from Evans et al. (2009) and Winkelmann et al. (2010) identified mega-scale glacial lineations and recessional moraines in patches along central Westwind Trough. These were interpreted as recording a grounded GrIS that extended to at least as far as the mid-shelf as a fast-flowing palaeo-ice stream, which underwent subsequent episodic retreat. Moraines on the adjoining shallow banks were interpreted as a product of grounded, non-streaming, ice. Although undated, a last glacial age for these landforms was inferred on the basis of their well-preserved nature. A shelf-edge extent for the last ice sheet was inferred indirectly from the presence of glacial sediments in the form of gravity flow deposits on the adjoining continental slope (Evans et al., 2009).

Subsequent mapping of seafloor landforms identified mega-scale glacial lineations that extended to the shelf-edge in both Norske and Westwind troughs, as well as large grounding-zone wedges on the mid-shelf (Arndt et al., 2015; Arndt, 2015). The lineations were incised into an acoustically transparent sediment unit with a sharp basal reflector interpreted as a subglacial till (cf. Evans et al., 2009). Collectively the seafloor geomorphology and acoustic stratigraphic evidence was interpreted as recording streaming flow to the shelf-edge in both troughs during the LGM, but with a more restricted ice sheet on the intervening shallow banks, terminating inshore of the shelf-edge (Arndt, 2015). Further south, in Store Koldewey Trough, streamlined glacial landforms and basal till in sediment cores were similarly interpreted to record the former presence of grounded, streaming ice that terminated at the shelf-edge (Laberg et al., 2017; Olsen et al., 2020). Grounding-zone wedges and recessional moraines record episodic ice stream retreat along the trough and deglacial lithofacies in sediment cores show that this retreat occurred in a glacial marine environment (Olsen et al., 2020). Collectively therefore these marine geophysical and sedimentological data indicate an extensive GrIS which advanced to the shelf-edge in several of the major cross shelf troughs offshore of northeast Greenland. However, the inference of a LGM age for this advance has, to date, been more circumspect and was primarily based on the well-preserved nature of the landforms and the absence of a thick postglacial sediment drape.

More recently Rasmussen et al. (2022) studied a sediment core recovered from the shelf-edge south of the mouth of Westwind Trough at 79.4°N. These authors utilised foraminiferal abundance, sedimentology and geochemistry, combined with AMS radiocarbon dating, to reconstruct GrIS extent and palaeoceanography during and following the LGM. The dates indicate that the core preserves a record from LGM (25.5 ka) to recent. The older part of the sequence comprises an iceberg

turbate with a well-preserved marine microfauna throughout the entirety of the LGM section. Rasmussen et al. (2022) argued that this provided evidence for a restricted GrIS which did not reach the shelf-edge in this location at the LGM.

There are no direct dating constraints on the timing of ice sheet advance or retreat from the shelf-edge to outer shelf in any of the major cross-shelf troughs offshore of northeast Greenland. Recent observations of GZWs in Norske Trough record grounding-line retreat to the mid-shelf prior to 16.6 ka BP (López-Quirós et al., 2024), which is a minimum for the timing of initial ice pull-back from the shelf edge. Onshore investigations from northeast Greenland using surface exposure dating and geomorphological mapping place the timing of initial ice sheet surface thinning to c. 22.9 ka (Roberts et al., 2024). Hence, while there is now an emerging picture of an extensive GrIS in the major troughs on the northeast shelf, a LGM interpretation for the age of this advance and the timing of initial retreat remain conjectural. The aim of this paper is therefore threefold: (1) to present new acoustic stratigraphic data and sediment cores from the mid- and outer shelf sectors of Westwind and Norske troughs; (2) to present new radiocarbon constraints on the timing of initial retreat of the GrIS from the shelf-edge offshore of northeast Greenland; and (3) to discuss the implications of these data for the ice sheet extent at the LGM, and the timing and rates of retreat.

2. Study area

The continental shelf offshore of northeast Greenland adjoins Fram Strait and is the widest part of the entire Greenland shelf at about 300 km in width (Fig. 1). Fram Strait is a major deep-water conduit for the exchange of warm Atlantic Water and cold Polar Water between the Arctic and North Atlantic. The East Greenland Current transports cold, low salinity surface water, icebergs and sea ice southwards to Denmark Strait, as well as Atlantic Intermediate water at depth. This warmer Atlantic water has been proposed as the driver for increased submarine melt rates and GrIS outlet glacier retreat (e.g., Straneo and Heimbach, 2013; Straneo et al., 2019; Wilson and Straneo, 2015; Mayer et al., 2018; Schaffer et al., 2020; von Albedyll et al., 2021).

The largest cross-shelf bathymetric troughs offshore of northeast Greenland are Norske and Westwind troughs (Arndt et al., 2015) (Fig. 1). These two troughs extend from the shelf-edge to the inner shelf where they connect and form a horseshoe-shaped arc around a shallower area of seafloor topography which includes the Belgica Bank and the Northwind Shoal. Westwind Trough is c. 300 km long, has an average width of c. 40 km and is about 300 m deep at the shelf-edge. From the shelf-edge and across the outer shelf the trough floor exhibits a relatively flat profile, a slight reverse bed from 300 to 250 km, then normal gradient across the inner shelf. Norske Trough has a length of c. 350 km; its width increases from 35 km on the inner shelf, to 90 km and 200 km on the mid-shelf and at the shelf-edge respectively (Arndt et al., 2015). In contrast to Westwind Trough, Norske Trough has a reverse gradient; water depths range from 320 m at the shelf-edge to over 500 m on the inner shelf (Fig. 1) Water depths across the intervening shallow banks are generally 20–100 m, with occasional deeper areas.

3. Data acquisition and methods

The marine geophysical and geological datasets were acquired during two cruises of the RV Polarstern to northeast Greenland in 2016 (PS100) and 2017 (PS109) (Alfred-Wegener-Institut, 2017). The data presented in this paper are from the middle and outer shelf parts of Westwind and Norske troughs including the continental shelf-edge and upper slope.

Information on seafloor morphology was acquired using a hull-mounted Teledyne RESON Hydrosweep DS3 multibeam system with a transmitting frequency of 15.5 kHz and a vertical depth accuracy of 0.5 % of the water depth. The multibeam data were collected continuously along the ships track during each cruise. The system was calibrated

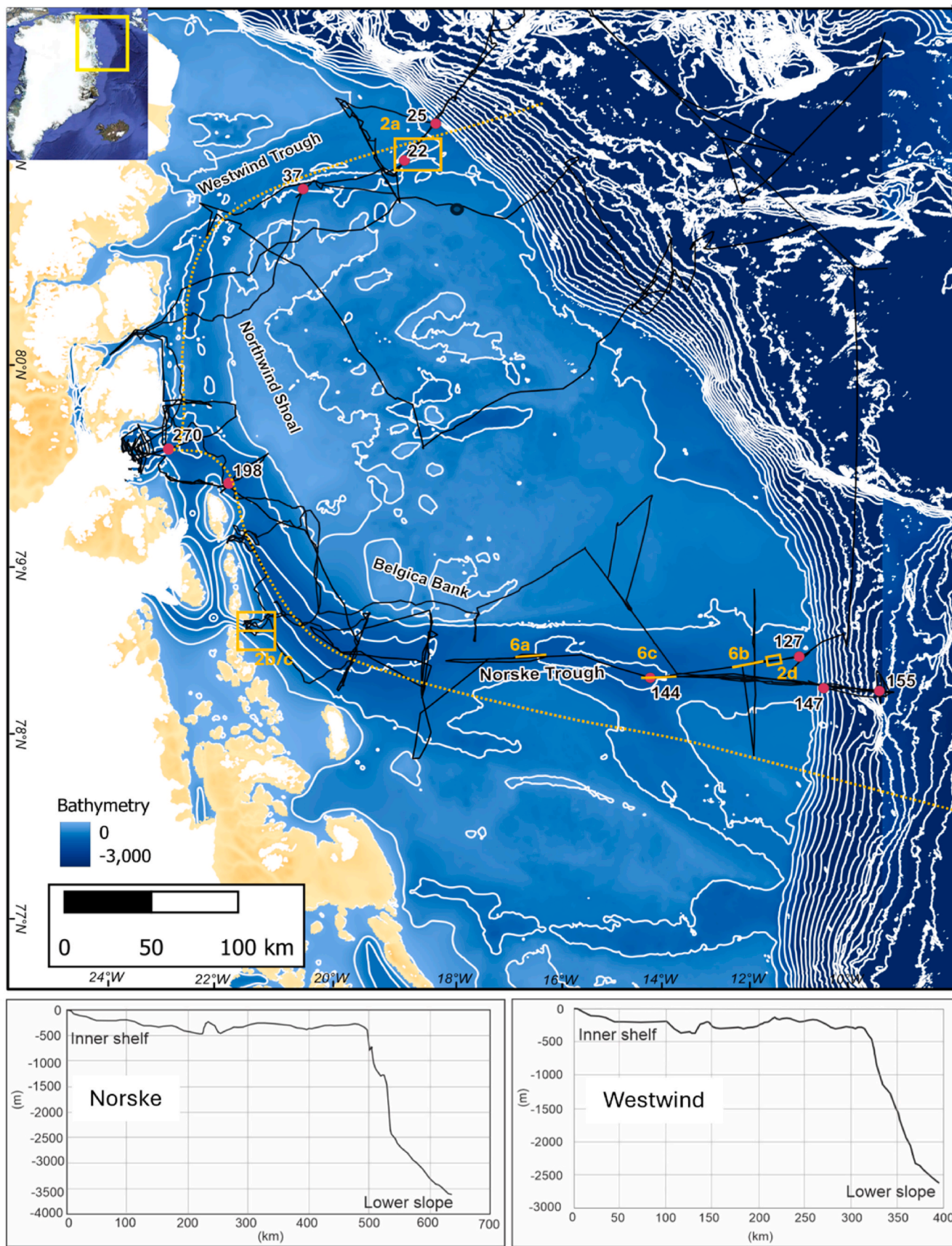


Fig. 1. Bathymetry of the continental margin adjoining NE Greenland, ship tracks along which geophysical data were collected (black lines) and locations of cores and figures referred to in text. Note Westwind Trough and Norske Trough are separated by the shallow areas of Belgica Bank and Northwind Shoal. Also shown in lower panels are topographic profiles along Norske and Westwind troughs extending from the continental slope to the inner shelf (marked as orange dotted lines in plan view). (For interpretation of the references to colour in this figure legend, the reader is referred to the Web version of this article.)

using sound velocity profiles from CTDs of the water column with data then cleaned and processed in CARIS HIPS and SIPS.

Sub-bottom profiler data on sediment thickness and acoustic stratigraphy were acquired using the hull-mounted PARASOUND system on the RV Polarstern. PARASOUND is a parametric system which employs two primary frequencies to generate a secondary pulse of lower frequency that is usually 5.5 kHz. Sub-seafloor penetration depth varies depending on the nature of the sediments but the system can penetrate up to c. 100 m of sediment with a vertical resolution of 0.3 m or better. The PARASOUND data were also used to identify suitable targets for sediment coring.

A gravity coring system was used to collect the sediment cores (Fig. 1 and Table 1). Barrel length was up to a maximum of 15 m but typically a barrel length of 5 m was used. Recovery was variable depending on the nature of the sediments. The sediment cores were used to sample different types of glacial, glaciomarine and marine sedimentary environments across the shelf and slope in order to establish the nature of glacial sedimentation. A key objective of the coring was to recover material that would determine the timing of ice sheet retreat from the shelf-edge using radiocarbon dating. Following recovery the sediment cores were cut into 1 m long sections and the cores then split and described according to the following criteria: colour, texture, sorting, sedimentary and deformation structures, bedding contacts, clast abundance and shape, macrofaunal content. Measurement of sediment shear strength in kPa was recorded using a hand-held Torvane. The cores were stored on ship and subsequently in Durham University at +4 °C. Additional information on sedimentary structures was obtained from the post-cruise examination of x-radiographs of the sediment cores using a GEOTEK MSCL-XCT scanner.

Samples of marine bivalves and benthic foraminifera were picked from the cores for radiocarbon dating. A total of 12 radiocarbon dates were acquired from cores on the mid- and outer shelf of Westwind and Norske troughs (Table 2). Wherever possible, sampling targeted lithofacies boundaries or, where the cores actually bottomed out in deglacial sediment, the base of the core in order to obtain a minimum age constraint on the timing of ice sheet retreat. Samples were dated at the Natural Environment Research Council Radiocarbon Facility (NRCF-East Kilbride).

The radiocarbon dates were corrected for isotopic fractionation and then calibrated to calendar years (cal a BP) using Calib 8.20 (Stuiver and Reimer, 1993) and the Marine20 radiocarbon calibration curve (Heaton et al., 2020). In calibrating the radiocarbon dates presented here we

Table 1
Location, water depth and recovery of sediment cores discussed in the text.

Core name	Location	Latitude (N)	Longitude (W)	Water Depth (m)	Core recovery (cm)
PS109/22-01-GC	Westwind Trough	80° 11.018	07° 26.587	329	265
PS109/25-01-GC	Westwind Trough	80° 14.371	05° 55.803	397	268
PS109/37-01	Westwind Trough	80° 21.873	10° 32.686	324	124
PS100/127-01 GC	Norske Trough	76° 45.549	7° 28.353	312	183
PS100/144-01 GC	Norske Trough	77° 7.495	10° 34.239	496	217
PS109/147-01	Continental slope offshore Norske Trough	76° 33.024	07° 29.261	628	295
PS109/155-01	Continental slope offshore Norske Trough	76° 21.402	06° 34.401	2030	201

follow the approach outlined in Heaton et al. (2023) for calibrating in polar regions. This takes into account the temporal uncertainties in the marine reservoir correction for high latitudes, specifically the larger reservoir correction needed for glacial periods. For radiocarbon dates with a calibrated age within the Holocene (taken here as starting from 11,500 cal a BP) we calculate ΔR and ΔR_{error} based on the 8 closest samples from the Marine Reservoir Correction Database (<http://calib.org/marine/>, Reimer and Reimer, 2001). This gives a marine reservoir correction ($\Delta R_{20}^{\text{Hol}}$) of 2 ± 66 used in calibration (Table 2). For pre-Holocene aged samples we perform two calibrations to provide a more realistic estimate of the age and age uncertainty. The first calibration assumes minimal polar ^{14}C glacial depletion and uses the $\Delta R_{20}^{\text{Hol}}$ estimate as above. The second calibration uses an estimated latitude-dependent maximal polar ^{14}C glacial depletion from Heaton et al. (2023). This is added to the Holocene value to give the glacial correction: $\Delta R_{20}^{\text{GS}}$. We then take the conservative approach of using the full calibrated range from these two calibrations to calculate the median and range of ages used in the discussion (all calibrations are shown in Table 2).

4. Acoustic and sedimentary data

4.1. Westwind Trough - results

4.1.1. Acoustic data

Previous bathymetric studies in mid-to outer Westwind Trough have identified seafloor areas characterised by mega-scale glacial lineations and recessional moraines (Evans et al., 2009; Winkelmann et al., 2010; Arndt et al., 2015, 2017). Data collected during 2016 and 2017 on cruises PS100 and PS109 support these observations and show mega-scale glacial lineations in the outer shelf trough that are orientated parallel and sub-parallel to the trough long-axis (Fig. 2a). The lineations have amplitudes of c. 3m and are formed in an acoustically transparent sediment unit.

At the shelf-edge a sediment wedge occurs in 375–400 m water depth (Fig. 3a). The wedge is composed of acoustically semi-transparent and structureless sediment, 10–15 m thick, with a discontinuous basal reflector. It tapers seawards and overlies an acoustically transparent to semi-transparent structureless unit with a strong upper reflector and no visible basal reflector. Core PS109-25 was recovered from the seaward end of the wedge in a water depth of 397 m (Fig. 3a).

Two further sediment wedges are imaged in the sub-bottom data inshore of PS109-25. The more inshore of the two wedges is 1.9 km in length and up to 12 m thick. A second wedge occurs seaward and is c. 2 km in length and c. 9 m thick (Fig. 3b). Sediment core PS109-22 was recovered from the seaward end of this second wedge. Internally the wedges consist of acoustically semi-transparent sediment with some weak internal reflectors. The wedges have a prominent seabed reflector that is incised in places by v-shaped depressions (Fig. 3a). They taper down-trough and overlie a massive semi-transparent to transparent acoustic unit with a sharp upper reflector.

4.1.2. Sedimentary data

Core PS109-25 is situated at the eastern end of Westwind Trough in 397 m water depth (Fig. 1). It is 268 cm long and contains three main lithofacies. The lowermost lithofacies is 42 cm thick, and extends from the core base to 226 cm depth. It is a massive, matrix-supported, muddy dark brown (10 YR 4/2) diamicton, which is relatively clast-rich with subangular-subrounded clasts up to pebble size. Shear strength ranges from 10 to 20 kPa (Fig. 4). The massive diamicton grades upwards into stratified, clast-rich, matrix-supported diamicton from 226 to 138 cm core depth (Fig. 5a). The matrix of the latter varies from clay-rich to silt-rich and it contains subangular to subrounded, occasionally striated, clasts. Its colour varies from dark greyish brown (2.5 YR 4/2) to dark brown (10 YR 4/3–4/2). Stratification is imparted by textural variation in the matrix, as well as locally, more pronounced laminae and beds (up

Table 2

Radiocarbon dates from sediment cores discussed in the text. Estimation of marine reservoir correction follows the approach outlined for polar regions in Heaton et al. (2023). ΔR and ΔR_{error} for marine reservoir correction used in calibrating Holocene aged samples is estimated based on average of 8 nearest points from the radiocarbon reservoir correction database (Reimer and Reimer, 2001) giving a value for $\Delta R_{20}^{\text{Hol}}$ of 2 ± 66 . For pre-Holocene samples the maximal ^{14}C glacial depletion is taken from Heaton et al. (2023) and added to $\Delta R_{20}^{\text{Hol}}$ to produce the glacial correction ($\Delta R_{20}^{\text{GS}}$). We then use the combined range and median age of that range in the discussion.

Laboratory code	Core	Depth (cm)	Sample type	^{14}C age $\pm 1\sigma$ (yrs BP)	Calibrated Age using $\Delta R_{20}^{\text{Hol}}$ (cal yrs BP)(2 σ upper and lower range)	$\Delta R_{20}^{\text{GS}}$	Calibrated Age GS (cal yrs BP) (2 σ upper and lower range)	Calibrated age combined range and median
UCIAMS-216442	PS100-127	6–10	Mixed benthic foraminifera	19160 \pm 60	22236 (21965–22488)	872 \pm 66	21175 (20841–21543)	21664 (20841–22488)
UCIAMS-216444	PS100-127	40–44	Mixed benthic foraminifera	19020 \pm 70	22102 (21815–22367)	872 \pm 66	21001 (20678–21360)	21522 (20678–22367)
UCIAMS-216445	PS100-127	133–134	Mixed benthic foraminifera	30630 \pm 250	34276 (33741–34791)	872 \pm 66	33425 (32774–34069)	33782 (32774–34791)
SUERC-76493	PS100-127	172–173	Mixed benthic foraminifera	15146 \pm 49	17517 (17203–17846)	872 \pm 66	16438 (16135–16758)	16990 (16135–17846)
UCIAMS-210585	PS100-144	72–73	Mixed benthic foraminifera	9370 \pm 70	10003 (9663–10271)			
SUERC-76494	PS100-144	104–105	Mixed benthic foraminifera	13622 \pm 44	15586 (15284–15887)	832 \pm 66	14361 (14046–14771)	14966 (14046–15887)
UCIAMS-210586	PS100-144	174–175	Mixed benthic foraminifera	16520 \pm 120	19042 (18705–19420)	832 \pm 66	18184 (17800–18572)	18610 (17800–19420)
UCIAMS-216449	PS109-22	44–45	Mixed benthic foraminifera	9625 \pm 30	10345 (10136–10578)			
SUERC-80919	PS109-25	137–138	Lima hyperborean valve	16897 \pm 50	19485 (19179–19808)	762 \pm 66	18636 (18309–18863)	19058 (18309–19808)
UCIAMS-211074	PS109-25	218–219	Mixed benthic foraminifera	38230 \pm 820	41646 (40553–42534)	762 \pm 66	41182 (39925–42179)	41229 (39925–42534)
UCIAMS-211077	PS109-37	61–65	Mixed benthic foraminifera	13070 \pm 70	14839 (14410–15183)	762 \pm 66	13666 (13412–13975)	14298 (13412–15183)

to a few cm thick) of mud and sandy mud (Fig. 5a). Occasional discrete laminae of silt and clay up to 0.3 cm thick, and lacking clasts, are also present. Contacts with the surrounding diamicton range from sharp to gradual. Shear strength within the stratified diamicton range from 9 to 17 kPa (Fig. 4). The stratified diamicton grades upwards into 9 cm of dark grey to dark greyish brown (2.5 YR 4/2–4/3) massive silty clay with a shear strength of 2 kPa. The upper 130 cm of the core comprises initially stratified and then massive clayey silt with dispersed pebbles and granules and darker mottled patches (Fig. 4). Shear strength through this uppermost unit ranges from 0.6 to 5.8 kPa (Fig. 4), and colour ranges from brown to dark yellowish brown (10 YR 4/4 - 4/3 - 4/2). The darker mottles are very dark grey (10 YR 3/1).

Two samples for radiocarbon dating were obtained from core PS109-25. A sample of mixed benthic foraminifera from 218 to 219 cm depth within the stratified diamicton dated 41229 cal a BP (UCIAMS-211074) (Fig.5a). A second sample from 137 to 138 cm comprised a single *Lima hyperborean* valve from the unit of massive silty clay that overlies the stratified diamicton (Fig. 4). This dated 19058 cal a BP (SUERC-80919) (Fig. 4 and Table 2).

Core PS109-22 was collected in 329 m water depth about 30 km from the shelf edge (Fig. 1). It is 256 cm long and the majority of the core (256–53 cm depth) comprises a massive, matrix-supported and clast-rich diamicton. Clasts are subrounded to angular and are dispersed in a silty clay matrix. Matrix colour ranges from brown (7.5 YR 4/2–10 YR 5/3) to grey (7.5 YR 5/1) to reddish brown (5 YR 4/3) with gradational colour transitions. Shear strength ranges from 0 to 9.4 kPa but generally decreases upwards (Fig. 4). From 160 to 124 cm depth clasts within the diamicton form aligned and inclined lineaments (Fig. 5b). There is also some localised stratification present due to thin (0.3–0.4 cm thick) sandy laminae with gradual boundaries at 124–122 cm depth. From 53 to 46 cm depth the massive diamicton grades into a more stratified diamicton. Stratification is imparted by textural banding, is discontinuous and, in places, almost indistinct. The stratified diamicton grades upwards into 10 cm of stratified gravelly mud which is, in turn, overlain by 38 cm of massive, dark greyish-brown (10 YR 4/2) clast-poor, silty clay (Fig. 4)).

Shear strengths in the stratified diamicton vary between 2.5 and 4 kPa. The silty clay is predominantly massive, although in places there are diffuse boundaries reflecting slight textural changes. A sample of mixed benthic foraminifera from the stratified gravelly mud at 44–45 cm depth dated 10345 cal a BP (UCIAMS-216449) (Table 2 and Fig. 4).

Core PS109-37 was collected from the mid-shelf section of Westwind Trough about 92 km from the shelf edge (Figs. 1 and 4). The core was recovered from an acoustically-transparent sediment unit sitting over a strong basal reflector in 325 m water depth (Fig. 3c). The lower part of the core from 106 to 75 cm depth, comprises a massive, matrix-supported, muddy, dark grey (10 YR 4/1) diamicton with dispersed clasts in a silty matrix (Fig. 5c). There is some faint stratification in its uppermost 5 cm. Shear strengths within the diamicton increase with depth and range from 3.4 to 11.6 kPa. From 75 to 63 cm depth the massive diamicton is overlain by crudely stratified, dark greyish brown (2.5 YR 4/1–4/2), pebbly mud with sharp upper and lower contacts. Stratification is gently inclined and is imparted by variable clast concentrations and textural variation (Fig. 5c). The upper contact of the stratified diamicton is relatively sharp. The upper 63 cm of the core comprises a clast-poor, silt/clay. Colour through this section of the core ranges from brown to dark greyish brown and dark grey (10 YR/1–4/2; 2.5 YR 4/1–4/1). The muds are massive with occasional gritty laminae and clasts. Shear strengths in these muds are 0–3.6 kPa (Fig. 4). A sample of mixed benthic foraminifera from 65 to 61 cm depth, and thus across the transition from the stratified muds into the overlying massive muds, dated 14298 cal a BP (UCIAMS-211077) (Table 2 and Fig. 4).

4.2. Norske Trough - results

4.2.1. Acoustic data

Well-developed streamlined landforms can be traced along Norkse Trough from the inner shelf to the shelf-edge (Fig. 2b and c). Arndt et al. (2017) mapped lineations in the northern sector of the mid-to outer-shelf trough. The lineations recorded are several tens of kilometres in length, are formed in an acoustically transparent sediment unit up to 20

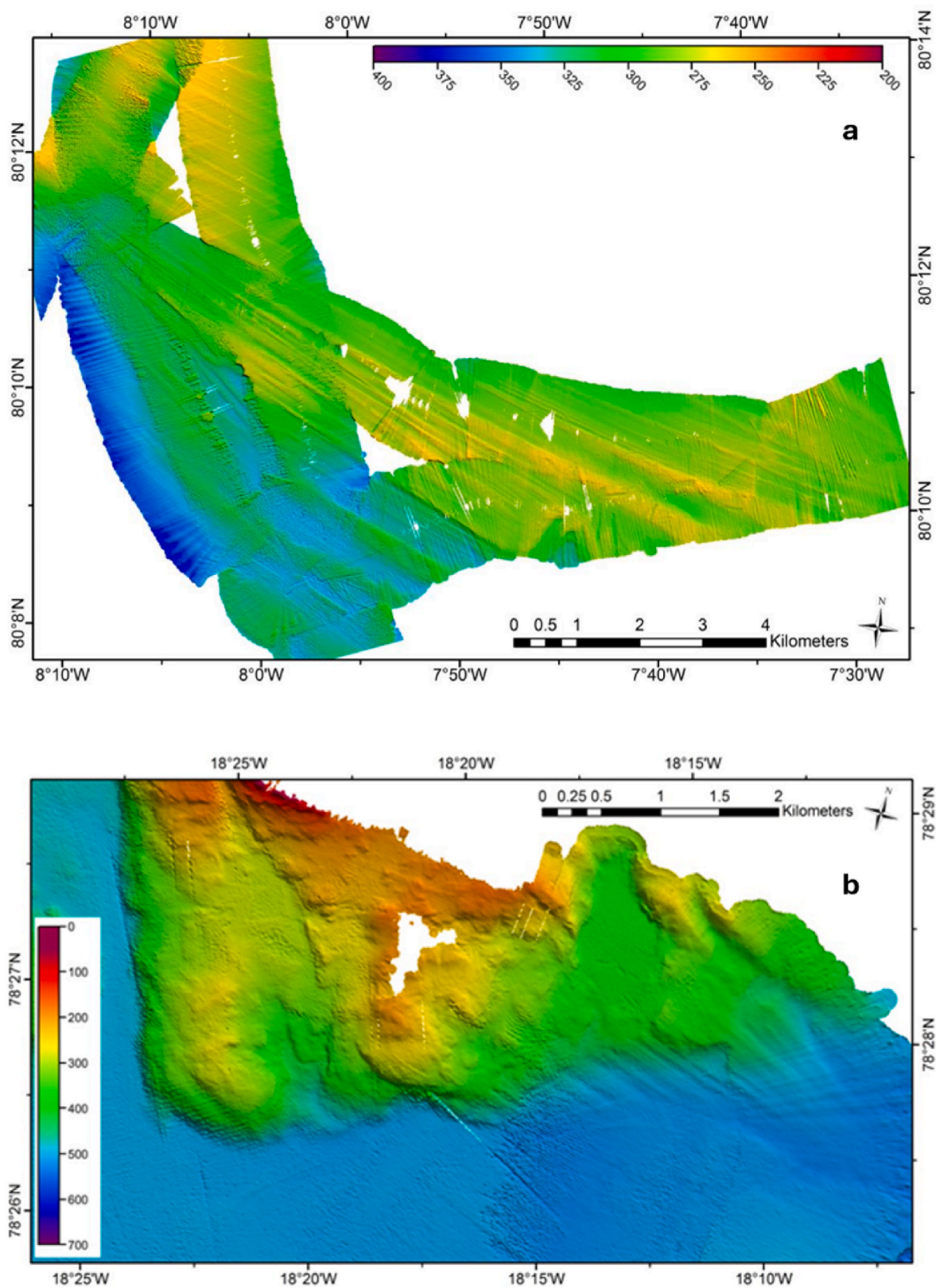


Fig. 2. Multibeam swath bathymetric images of streamlined landforms and ploughmarks on the sea floor of Westwind and Norske troughs. (a) Mega-scale glacial lineations from outer Westwind Trough; (b) and (c) Examples of streamlined seafloor bedforms Norske Trough; (d) Elongate rectilinear scours and ploughmarks incised into the seafloor of outer Norske Trough.

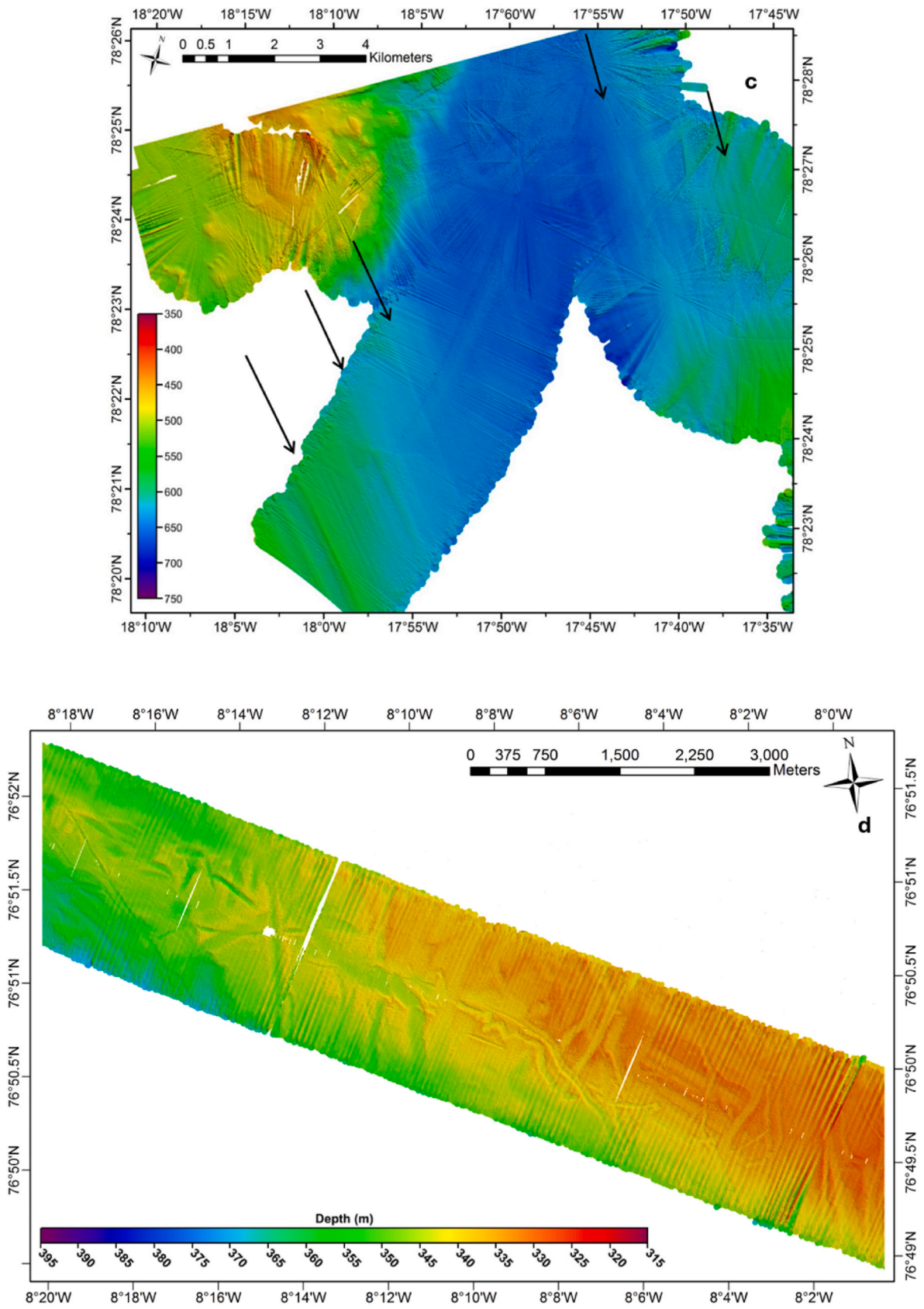


Fig. 2. (continued).

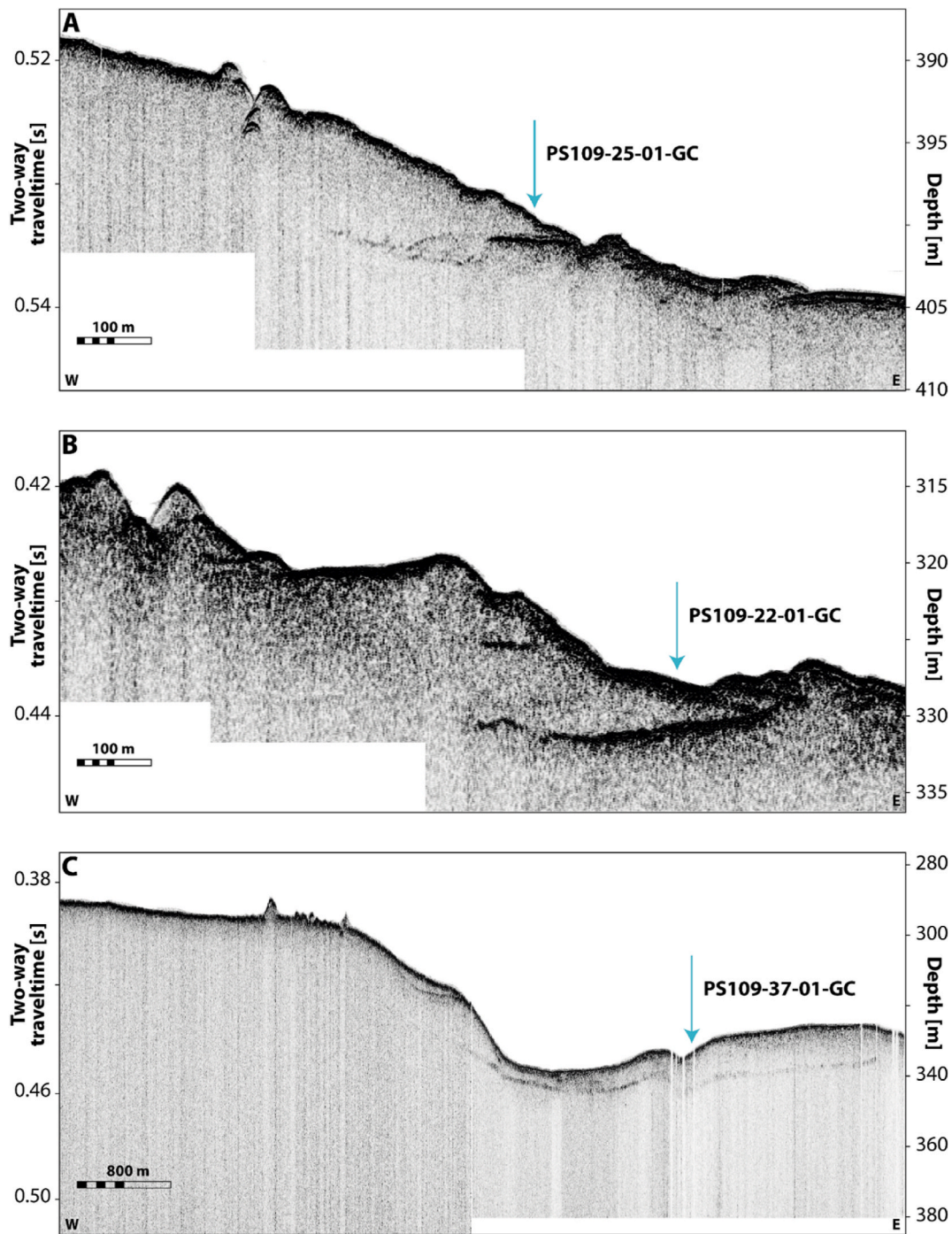


Fig. 3. Parasound records of subseafloor acoustic stratigraphy in outer Westwind Trough. (a) Shelf edge GZW showing location of core PS109-25. (b) GZW from outer Westwind Trough from which core PS109-22 was recovered. (c) Sediment wedge in middle Westwind Trough from which core PS109-137 was collected.

m thick, thinning to about 5 m at the shelf-edge, and which sit on top of a smooth and continuous basal reflector.

On the mid-shelf, a large 80 km long bathymetric sill is present in water depths as shallow as 360 m; this has been interpreted previously as a grounding-zone wedge (Arndt et al., 2015; López-Quirós et al., 2024). The seaward (down-trough) end of this sediment wedge consists of an acoustically homogeneous sediment unit with a strong basal reflector. The unit thickens inshore from 3 to 4 m in the toe of the wedge to about 17 m (Fig. 6a). It is overlain by a 1–2 m thick drape of acoustically transparent sediment at the distal edge of the wedge (Fig. 6a). The seafloor across much of outer Norske Trough is heavily dissected by rectilinear scours and plough marks which criss-cross the seafloor and

disturb the upper seafloor sediment (Fig. 2d).

Beyond the shelf-edge, on the adjoining continental slope, lenticular units of acoustically homogeneous sediment are present on sub-bottom profiler records down to water depths of over 2000 m (Fig. 7). These lenticular units are generally up to a maximum of 10 m thick, taper downslope and, in places, can be seen to occur in a stacked pattern.

4.2.2. Sedimentary data

Core PS100-127 was collected at the shelf-edge from an area of prominently iceberg-ploughed seafloor in 312 m of water (Figs. 1, 2d and 4 and 6b). The core comprises 1.83 m of matrix supported, silty-clay diamicton that is brownish-grey in colour. Structurally the diamicton is

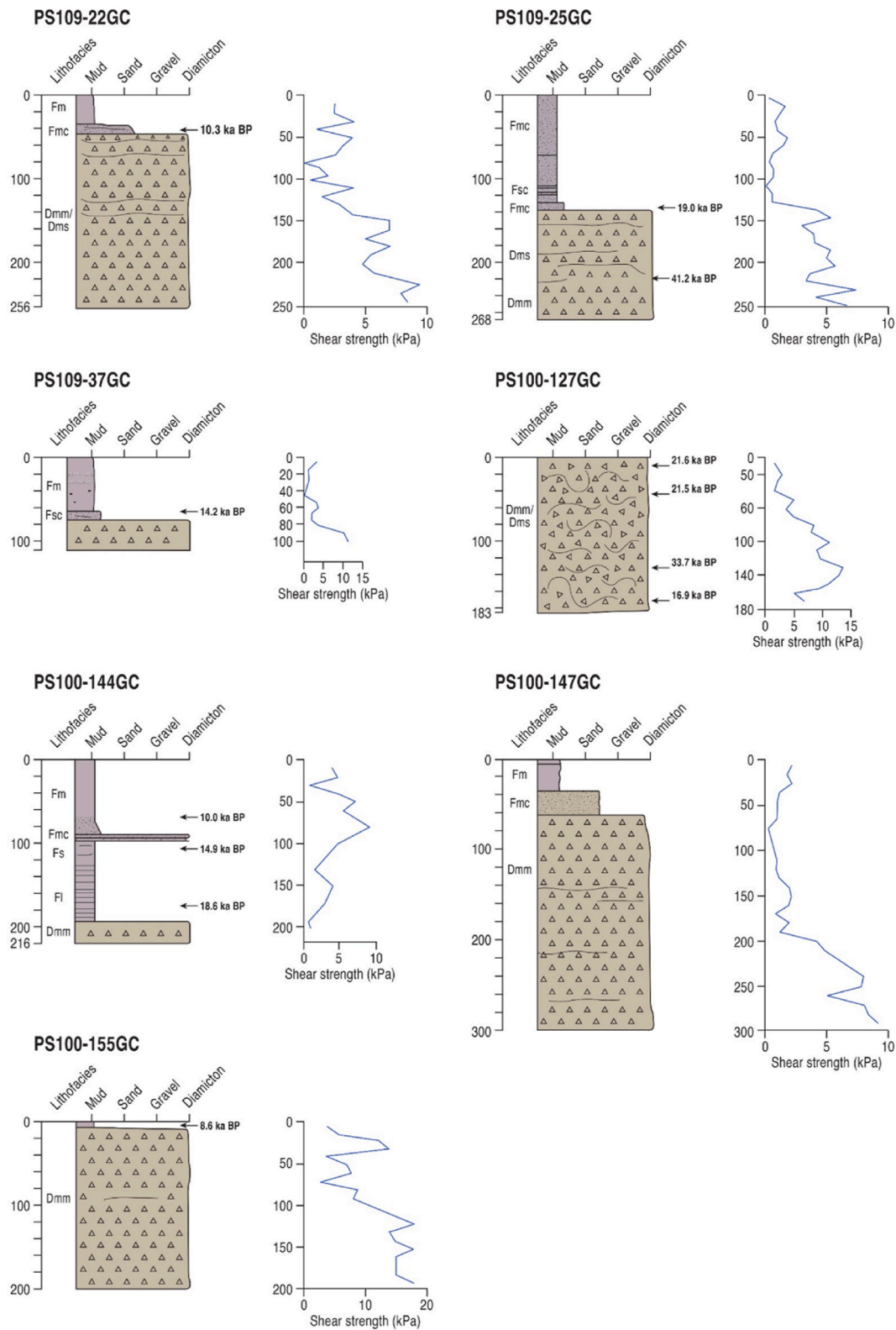


Fig. 4. Lithofacies logs, shear strength plots and radiocarbon dates of cores from Westwind Trough and Norske Trough as discussed in this paper.

predominantly massive with clasts dispersed in the matrix. However, the x-radiographs show that in some places it has a ‘swirled’ or chaotic appearance with dipping lineaments and clast alignments (Fig. 5d). Shear strength in the lowermost 20 cm of the core ranges from 5 to 6.8 kPa, increasing to 9–13.6 kPa from 155 to 100 cm before decreasing in the upper 70 cm from 1.5 to 5 kPa (Fig. 4).

Four samples comprising mixed benthic foraminifera were collected from PS100-127 for AMS radiocarbon dating. The dates are not in stratigraphic order and, from deepest to shallowest, are 16990 cal a BP (SUERC-76493), 33782 cal a BP, 21664 cal a BP (UCIAMS-216442) and 21522 cal a BP (UCIAMS-216444), respectively (Table 2 and Fig. 4).

Core PS100-144 was collected ~100 km inshore from the continental

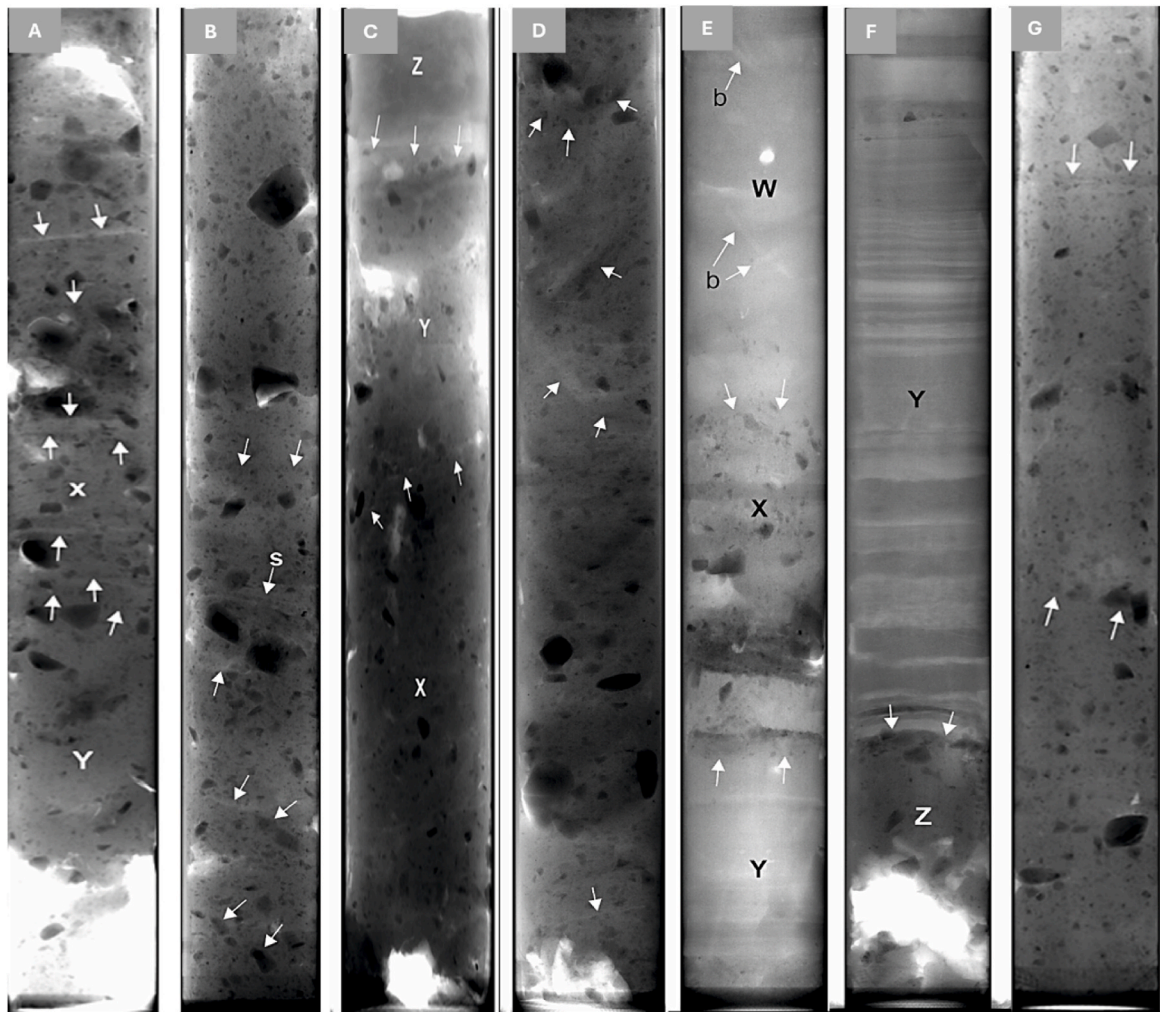


Fig. 5. X-radiographs of core lithofacies from Westwind and Norske troughs. (A) Core PS109-25, 168.5–268 cm depth. The lowermost 42 cm of the core comprises a massive, matrix-supported, clast-rich diamicton ('Y'). This is overlain gradationally by stratified, clast-rich, matrix-supported diamicton. Stratification (arrowed) is imparted by textural variations in the matrix and by the presence of laminations of mud and sandy mud. Contacts with the surrounding diamicton range from sharp to diffuse. (B) Core PS109-22, 65–160 cm depth. The x-radiograph shows massive, matrix-supported and clast-rich diamicton with subrounded to angular clasts dispersed in a silty clay matrix. In places there are inclined clast alignments and lineaments (arrowed) as well as very subtle stratification ('s'). (C) Core PS109-37, 56–106 cm depth. The lower 31 cm of the core comprises a massive, matrix-supported, muddy diamicton with dispersed clasts in a silty matrix ('X'). This is overlain by 12 cm of crudely stratified pebbly mud with relatively abrupt upper and lower contacts (arrowed). Note the gently inclined stratification. This stratified mud is overlain by 6 cm of clast-free massive silty and silty clay muds from 56 to 62 cm depth ('Z'). (D) Core PS100-127, 91–183 cm depth. Massive, matrix-supported diamicton with dispersed clasts. Occasional discontinuities and clast lineaments (arrowed) impart a locally developed 'swirled appearance to the sediment. (E) Core PS100-144, 46–116 cm depth. The lowermost ~118 cm of the x-radiograph shows laminated to stratified silty-clay muds with horizontal to sub-horizontal, planar parallel lamination ('Y'). These are overlain by c. 20 cm of more gritty, massive to crudely stratified muds with abundant granules, sand and occasional pebbles ('X'). The base and top (arrowed) of this more clast-rich facies are respectively sharp and gradational. The upper 29 cm of the x-radiograph is characterised by massive, silty clay ('W') with occasional zoophycos burrows ('b'). (F) Core PS100-144, 116–216 cm depth. The lowermost 26 cm of the x-radiograph comprises a massive, matrix-supported diamicton ('Z') which is overlain sharply (contact is arrowed) by 74 cm of laminated silty clay with planar, parallel, horizontal to sub-horizontal laminae. (G) Core PS109-147, 96–196 cm depth. Massive matrix-supported diamicton with dispersed clasts in a silty clay matrix. The diamicton appears largely structureless with only occasional discontinuities and clast alignments (arrowed).

shelf-edge in 496 m water depth (Figs. 1, 4 and 6c; Table 1). From the base of the core at 216 cm–190 cm the sediment comprises a 26-cm thick unit of very dark grey (5 YR 3/1), massive, matrix-supported diamicton (Fig. 5e). Shear strengths in the diamicton are low (0.8–1 kPa). This is overlain sharply by almost 100 cm of dark greyish brown, laminated silty clay grading into stratified silty clay in its uppermost 30 cm. Lamination is generally planar, horizontal to sub-horizontal and reflects changes in grain size from silty to more clay-rich horizons (Figs. 4 and 5e). Shear strengths through these muds range from 1.5 to 4 kPa. From 98.5 to 78 cm depth the laminated and stratified muds are replaced sharply by slightly stiffer (7.5 kPa) and more gritty, massive to crudely stratified muds with abundant granules and sand and occasional pebbles (Fig. 4). The gritty muds have a sharp lower contact and grade upwards

into 49 cm of dark grey (7.5 YR 4/1) massive silty clay which is gritty towards the base. The upper 29 cm of the core comprises massive, silty clay that is mottled in places, contains occasional siltier pods and clay laminae, has a shear strength of 3.4–4 kPa and is predominantly brown to dark greyish brown in colour (10 YR 3/3, 10 YR 4/3, 2.5 YR 3/2 and 10 YR 4/2) (Fig. 4).

Three samples comprising mixed benthic foraminifera were collected from PS100-144 for AMS radiocarbon dating (Table 2 and Fig. 4). A sample from 175 to 174 cm depth, within the laminated mud facies and 14–15 cm above the contact with the underlying massive diamicton, dated 18610 cal a BP (UCIAMS-210586). A second sample from 105 to 104 cm depth towards the top of the laminated-stratified muds dated 14966 cal a BP (SUERC-76494). A final sample from 73 to 72 cm depth

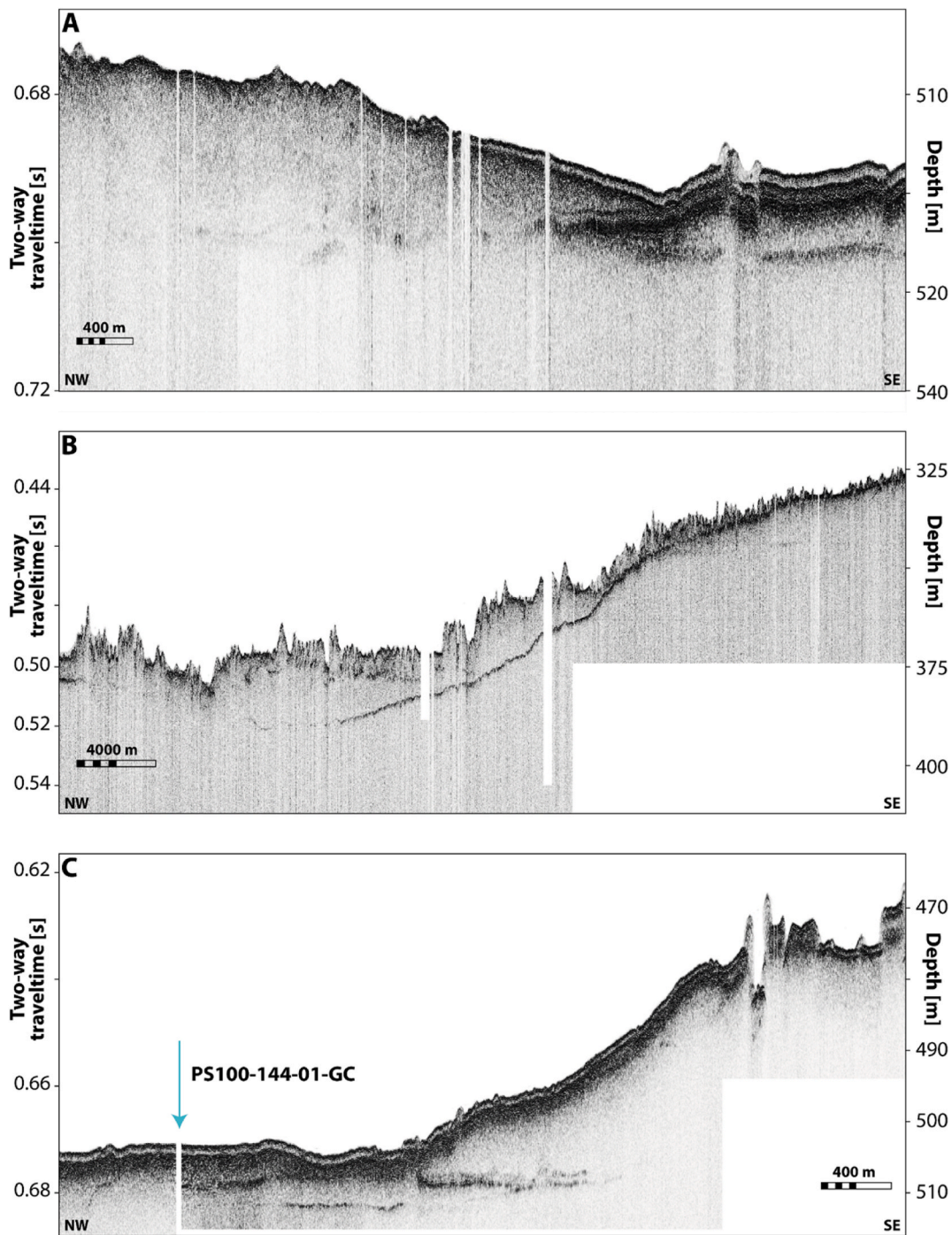


Fig. 6. Parasound records of subseafloor acoustic stratigraphy mid-outer Norske Trough. (a) GZW middle Norske Trough. Ice flow was from left to right in the image. Note the prominent wedge shape and acoustically transparent layer which stratigraphically overlies the wedge. (b) Iceberg ploughed seafloor outer Norske Trough. (c) Parasound record of core site PS100-144.

and 5–6 cm above the upper contact with the massive gritty mud dated 10003 cal a BP (UCIAMS-210585).

Sediment cores collected from the lenticular units of acoustically homogeneous sediment on the upper and lower slope (cores PS109-147-01-GC and PS109-155-01-GC from 644 m to 2030 m water depth respectively) bottomed out in 1–2 m of dark grey (10 YR 3/1-10 YR 4/1-10 YR 4/2) massive, matrix-supported, diamicton with dispersed clasts in a silty clay matrix (Fig. 5g). Shear strengths in this diamicton facies characteristically increase downcore and range from 0.8 to 18 kPa (Fig. 4). A sample of mixed benthic foraminifera from 8 to 9 cm depth in core PS109-155-01-GC dated 8462 cal a BP (SUERC-79889).

4.3. Westwind Trough – data interpretation

Streamlined landforms in the form of mega-scale glacial lineations formed in sediment and aligned parallel or sub-parallel to the axis of Westwind Trough have been described in several previous studies and were interpreted as a product of grounded, streaming ice, flowing along the trough to the shelf-edge (Evans et al., 2009; Arndt et al., 2015, 2017). Similar landforms characterise many high-latitude shelf troughs and are typically related to the former presence of palaeo-ice streams (e. g., Ó Cofaigh et al., 2002, 2013a; Graham et al., 2009; Hogan et al., 2016; Olsen et al., 2020). In the case of Westwind Trough they indicate

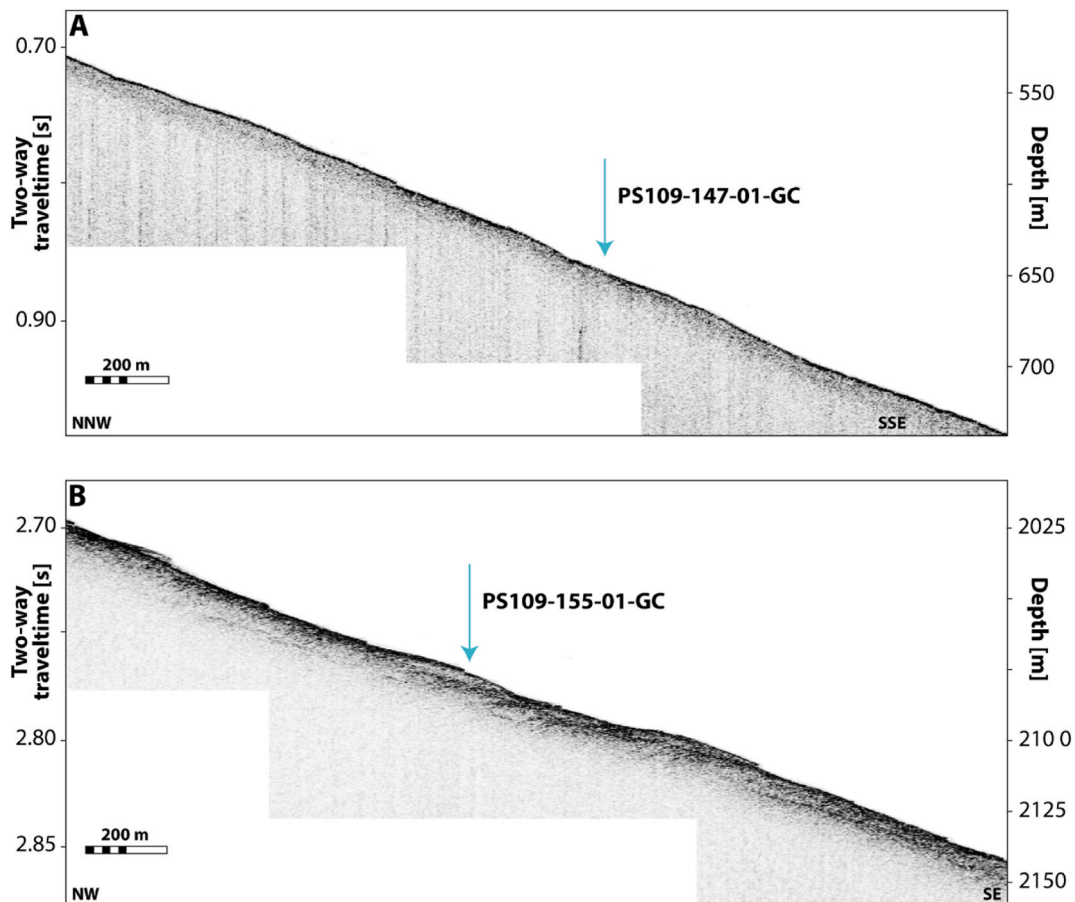


Fig. 7. Parasound records from continental slope adjoining Norske Trough. (a) Location of core PS109-147-01-GC. (b) Location of core PS109-155-01-GC. Note lenticular acoustic units interpreted as glaciogenic debris flows (see text).

an extensive GrIS that was grounded to the shelf-edge.

The outer shelf sediment wedges, including one at the shelf-edge, are characterised by an acoustically semi-transparent and homogeneous internal structure, a strong basal reflector, as well as a distinctly tapered distal end (Fig. 3). Occasional internal reflectors imply there may be variation in sediment physical properties and/or layering, suggesting, in turn, incremental sediment deposition. The semi-transparent and homogeneous internal structure suggests the features are composed of diamicton (Ó Cofaigh et al., 2005; Dowdeswell and Fugelli, 2012; Batchelor and Dowdeswell, 2015), and this is confirmed by the sediment cores from these wedges (see above). Hence, these landforms bear similarities to grounding-zone wedges described from the literature on glaciated continental shelves (Batchelor and Dowdeswell, 2015; Callard et al., 2018; Bradwell et al., 2019; Ó Cofaigh et al., 2021). However, classic grounding-zone wedges are usually characterised by a distinct ‘ramp-step’ profile which consists of a gentler ice-proximal ramp, and steeper, ice-distal, scarp face. This morphology reflects increased accommodation space with distance from the grounding line in an ice shelf cavity. As such these landforms are thought to be indicative of the former presence of an ice shelf.

In the case of the wedges from Westwind Trough, the tapering down-trough form, combined with the presence of internal reflectors and their diamictic composition, suggests formation by the progradation of poorly-sorted, diamictic sediment, in a down-ice direction. As such, we infer that the sediment wedges in Westwind Trough, while not being classic grounding-zone wedges (*sensu stricto*) (cf. Batchelor and Dowdeswell, 2015), were nonetheless produced at the grounding line and reflect the advection of poorly sorted, glaciogenic sediment to the grounding line and beyond. Internal reflectors and an overall tapered

profile suggests that debris flow processes were likely involved in their formation (Dowdeswell and Fugelli, 2012; Batchelor and Dowdeswell, 2015). The tapered profile of the Westwind Trough sediment wedges further implies that their formation was not constrained by an ice shelf cavity. Their low amplitude (c. 9–15 m thick) is an order of magnitude smaller than the current cavity depth of c. 500 m beneath the floating tongue of 79N Glacier (Lindeman et al., 2020; Schaeffer et al., 2020). Hence, it is possible that while these sediment wedges are grounding-zone features associated with an ice shelf, it is equally possible that they were produced at a retreating tidewater glacial margin.

Core PS109-25 was recovered from the shelf-edge sediment wedge (Fig. 3). The core bottomed out in a massive diamicton which grades upwards into stratified diamicton and then massive silty clay (Fig. 4). We infer this sequence to record sedimentation in a progressively subglacial to deglacial environment with the lowermost massive diamicton with shear strengths up to 20 kPa representing a subglacial till and the overlying stratified diamicton with striated clasts most likely recording grounding-line proximal deposition from subaqueous, cohesive debris flows. The latter interpretation is supported by the presence of textural banding as well as laminae and beds within the matrix-supported stratified diamicton (Eyles and Eyles, 2000; Mulder and Alexander, 2001; Talling et al., 2012). The overlying massive silty clay is interpreted to record suspension settling of fine-grained glacial marine sediment in a more ice distal glacial marine setting following grounding line retreat, with the brown to yellowish-brown mottled mud above representing hemipelagic sedimentation in an open-marine setting. The darker mottled patches are most likely a product of bioturbation.

Two dates were obtained from this core (Table 2 and Fig. 4). The

lower date on mixed benthic foraminifera was from the stratified diamicton facies and dated 41.2 cal ka BP. This provides a maximum age for formation of the stratified diamicton but is quite possibly non-finite (Walker, 2005). A second date on an intact valve of *Lima hyperborean* from the silty clay that overlies the stratified diamicton dated 19.0 cal ka BP. This constrains the timing of ice-distal glacial marine sedimentation following grounding-line retreat and is thus a minimum age for initial retreat of the GrIS from the shelf-edge in Westwind Trough.

Subsequent grounding-line retreat in Westwind Trough is constrained by a date of 14.3 cal ka BP from core PS109-37 from the mid-shelf trough (Figs. 1, 3 and 4; Table 2). The upwards transition from massive, matrix-supported diamicton into crudely stratified, pebbly mud, and then massive mud, is once again inferred to record a subglacial to deglacial sequence with the stratified mud representing initial grounding-line retreat and transition to a deglacial setting. The date of 14.3 cal ka BP from the stratified mud provides a minimum age for GrIS retreat in mid- Westwind Trough.

4.4. Norske Trough – data interpretation

Streamlined lineations formed in sediment and orientated parallel and sub-parallel to the long-axis of Norske Trough record former flow of grounded ice to the shelf-edge, most likely as a fast-flowing palaeo-ice stream (cf. Ó Cofaigh et al., 2002; Ottesen and Dowdeswell, 2009; Graham et al., 2009; Arndt et al., 2017). A shelf-edge position is also implied by the lenses of acoustically homogeneous sediment on the continental slope offshore of the mouth of Norske Trough (Fig. 7). The lenticular geometry of these units, their downslope tapering, stacked pattern and internal homogeneous structure are compatible with an origin as glacial debris flows delivered onto the continental slope from a shelf-edge terminating ice stream (Laberg and Vorren, 1995, 2000; Li et al., 2011). A glacial debris flow origin is also supported by the sediment cores which recovered dark-grey massive matrix-supported diamictons from the slope (Fig. 7) (Elverhøi et al., 1997; Laberg and Vorren, 2000; Ó Cofaigh et al., 2013b; Ó Cofaigh et al., 2018).

The stratigraphy and lithofacies preserved in core PS100-144 (Fig. 4) are interpreted as recording a glacial-deglacial sequence in outer Norske Trough. The lowermost unit in the core comprises a massive, matrix-supported diamicton with very low shear strengths (0.8–1 kPa). Massive diamictons in glacial environments can be produced by a range of processes including subglacial till formation, cohesive debris flow deposition and iceberg rafting and turbation (Dowdeswell et al., 1994; Eyles and Eyles, 2000; Evans, 2018). The low shear strengths imply the diamicton has not been over-consolidated. Such low shear strengths might be consistent with subaqueous sedimentation either in the form of an iceberg-rafted deposit or debris flow during grounding-line retreat. However, weak subglacial tills associated with former palaeo-ice streams have been documented in polar cross-shelf bathymetric troughs (e.g., Dowdeswell et al., 2004; Ó Cofaigh et al., 2007); hence the shear strengths are not conclusive. We return to the origin of the basal diamicton below.

The facies sequence indicates a marked change in sedimentation above the diamicton with the transition to laminated, and then stratified, silty clay. The planar and horizontal to sub-horizontal nature of the lamination suggests that these deposits are a product of meltwater sedimentation with suspension settling of fine-grained sediment through the water column from turbid plumes (Mackiewicz et al., 1984; Powell and Domack, 1995; Ó Cofaigh and Dowdeswell, 2001; Lucchi et al., 2013; Streuff et al., 2017). However, clasts are rare within these laminated-stratified silty clays. Such clast-poor laminated muds have also been described from below the modern ice shelf in Petermann Fjord (Jennings et al., 2022) and have been documented in sub-ice shelf sedimentary systems more widely (e.g., Domack et al., 1999; Evans et al., 2005; Kilfeather et al., 2011; Smith et al., 2019). We infer that the laminated muds in PS100-144 were deposited in an ice shelf cavity

beyond the grounding line, such that the coarser-grained material melted out proximal to the grounding line during deglaciation, whereas finer-grained material was carried in suspension further, but still within the ice shelf cavity, before settling through the water column to produce the laminated muds.

The laminated and stratified muds are overlain sharply by a thin unit of poorly sorted, gritty mud with occasional pebbles. The sharp lower contact implies an abrupt change in depositional environment. This is also supported by a notably coarser component within the muds which suggest a marked change in the nature of sediment delivery to the core site reflected in a relatively abrupt increase in ice-rafted debris. We suggest that this reflects break-up of the fringing ice shelf and successive calving of icebergs from close to the grounding-line and rafting of coarse-grained subglacial sediment to the core site (cf. Pudsey and Evans, 2001; Lloyd et al., 2005; Kilfeather et al., 2011; Smith et al., 2019). The gritty muds transition upwards into massive silty clay, which becomes progressively more brown in colour vertically upwards and is mottled in places. Such mottling is most likely a product of bioturbation, which combined with the massive structure, implies a more distal glacial marine setting, most likely in an open-marine environment (cf. Jennings et al., 2018). The facies sequence preserved in core PS100-144 in Norske Trough therefore represents a progressive change in depositional environment from: (i) subglacial (or grounding-line proximal) to (ii) deglacial glacial marine below an ice shelf, to (iii) ice shelf break and then to (iv) open-marine conditions.

A date of 18.6 ka BP from the lower part of the laminated mud facies provides a minimum date for deglaciation of the core site and, thus, outer Norske Trough. Two further dates bracket the age of the ice shelf break up to between 15 ka BP and 10 ka BP (Fig. 4 and Table 2).

The massive, matrix-supported diamicton in core PS100-127 has a chaotic or 'swirled' appearance in places along with dipping and sub-horizontal lineaments (Figs. 4 and 5d). Shear strengths are variable (1.5–13.6 kPa). The core was collected from an area of iceberg-scoured seafloor close to the shelf-edge (Fig. 2d and 6b). This, combined with the massive and chaotic structure of the diamicton, is compatible with an origin as an iceberg turbate deposit (Dowdeswell et al., 1994). The chaotic and 'swirled' lineaments within the matrix are a direct product of deformation due to scouring and ploughing processes (Dowdeswell et al., 1994; Kilfeather et al., 2010).

The radiocarbon dates from the diamicton in PS100-127 record the timing of open marine conditions on the shelf. Importantly, however, they are out of stratigraphic order and are thus likely to be reworked. If the diamicton was a subglacial till, the youngest age of 17 cal ka BP would provide the best constraint on the timing of till formation and thus ice advance. However, core PS100-144 is located *inshore* of PS100-127 and has a deglacial date of 18.6 cal ka BP (see above). A subglacial till interpretation for the diamicton in core PS100-127 would therefore require an ice readvance over the site of PS100-144 in order to deposit a younger till at the shelf edge. There is no evidence of such a readvance across the site of PS100-144, and we therefore reinforce the interpretation that the chaotic deformation structures in PS100-127 are a product of iceberg turbation (Vorren et al., 1983; Barnes and Lien, 1988).

The four dates from PS100-127 record open marine conditions at the shelf edge and thus help to constrain the timing of the initial retreat of grounded ice in Norske Trough. As grounded ice was inshore of core site PS100-144 by 18.6 cal ka BP, the date of 17 cal ka BP from core PS100-127 must be younger than initial pull back of grounded ice from the shelf-edge. By 17 cal ka BP the shelf-edge was likely an ice distal glacial marine environment but was still receiving icebergs from a retreating GrIS further inshore in Norske Trough. We regard the date of 33.7 cal ka BP as too old for retreat of the last ice sheet from the shelf-edge of Norske Trough as this would imply the ice sheet took c. 15,000 years to retreat the c. 100 km from the shelf-edge to the site of core PS100-144. It is also unlikely given that initial retreat occurred much later at 19 cal ka BP in the adjacent Westwind Trough. Rather, dates of 21.6 and 21.5 cal ka BP

from PS100-127 are interpreted as providing the best constraint on deglaciation from the shelf-edge of Norske Trough as they indicate open-marine conditions at the shelf-edge at 21.6–21.5 cal ka BP. The turbation of this deposit occurred after that time as icebergs affected the seafloor substrate long after initial retreat.

5. Discussion

An extensive body of work from the continental shelf offshore of northeast Greenland shows strong evidence for a shelf-edge terminating, grounded ice sheet in several of the cross-shelf troughs in this region,

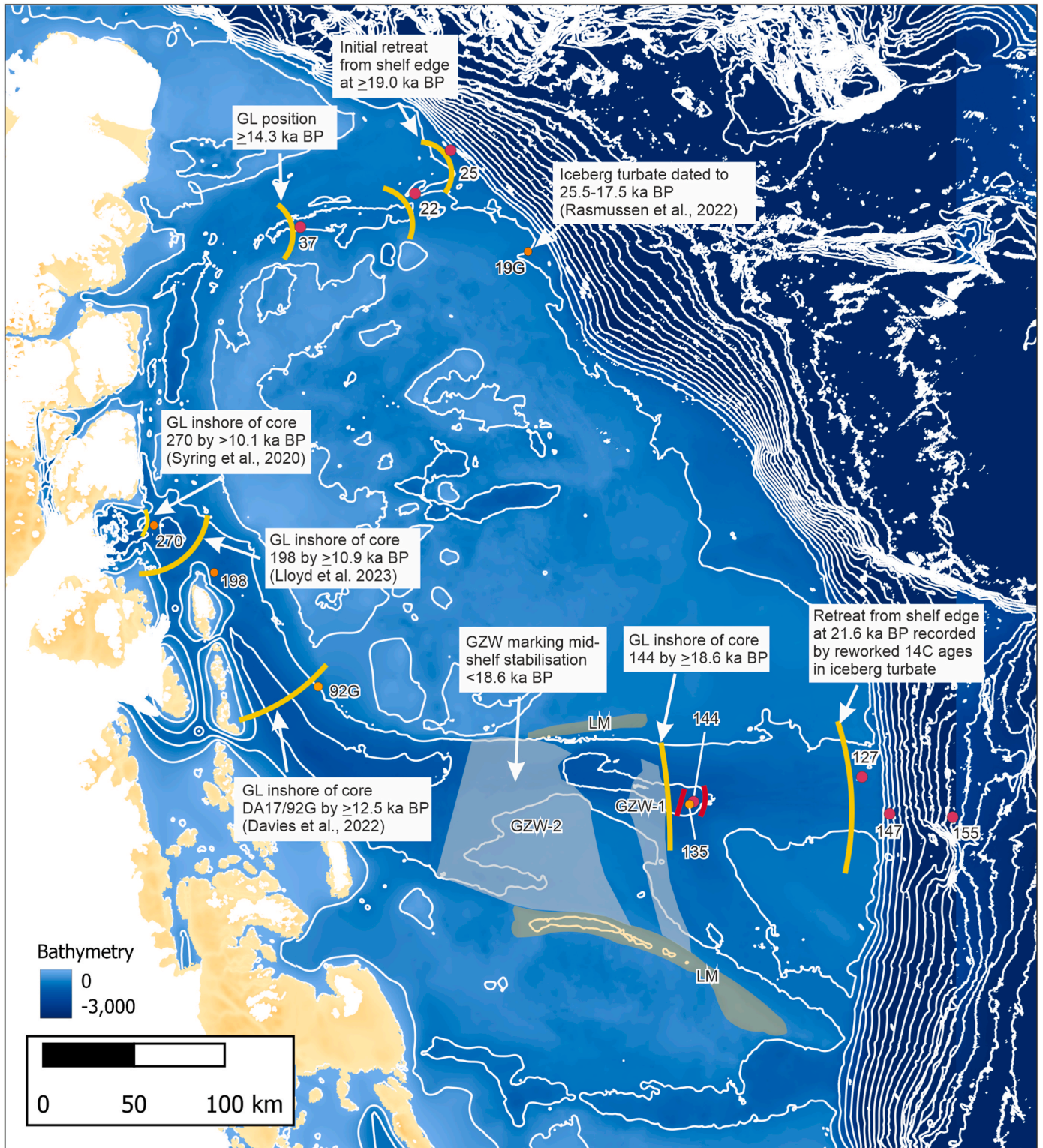


Fig. 8. Reconstruction of ice sheet extent at the LGM offshore NE Greenland and isochrones showing position of grounding line within Norske and Westwind troughs during deglaciation. ‘GZW-1’ and ‘GZW-2’ represent the positions and extents of grounding-zone wedges from the shelf and ‘LM’ represents the position of lateral moraines adjacent to Norske Trough (after [Arndt et al., 2015](#); [López-Quirós et al., 2024](#)). The location of additional cores is also shown: core 135 ([López-Quirós et al., 2024](#)), core 198 ([Lloyd et al., 2023](#)) and core 270 ([Syring et al., 2020](#)).

including Westwind and Norske troughs. This evidence typically comprises seafloor landforms in the form of flow parallel, streamlined, subglacial landforms, including mega-scale glacial lineations, as well as flow transverse features such as grounding-zone wedges and moraines (Evans et al., 2009; Winkelmann et al., 2010; Arndt et al., 2015, 2017; Laberg et al., 2017; Olsen et al., 2020; this study). The presence of these landforms in Westwind and Norske troughs are consistent with streaming flow in both troughs and thus an ancestral NEGIS which extended to the shelf-edge as a palaeo-ice stream. Indirect support for shelf-edge terminating ice is also present in the form of glacial debris flows from the continental slope offshore of the mouth of Norske Trough (Fig. 7). An extensive grounded ice sheet is further supported by sediment cores from the outer shelf in both troughs which bottomed out in subglacial till and/or poorly-sorted, proximal grounding-line, glacial sediments. The sedimentary, acoustic stratigraphic and geomorphological record from the outer shelf of both troughs therefore supports shelf-edge terminating, grounded ice. Although several previous studies have proposed that this most recent shelf-edge advance dates to the LGM (e.g., Arndt et al., 2017), until the present study there has been no direct chronological control from the Northeast Greenland shelf to support this.

The radiocarbon dates presented in this paper provide the first direct chronological constraint on the age of the most recent phase of shelf-edge terminating ice in Westwind and Norske troughs. They date the timing of initial ice sheet retreat from the shelf-edge and across the outer shelf in both troughs. In Westwind Trough a date from a shelf-edge, grounding-zone wedge indicates that retreat was underway by ≥ 19 cal ka BP, and the ice sheet had cleared the outer shelf by c. 14.3 cal ka BP (Fig. 8). In Norske Trough dates from an iceberg turbate at the shelf-edge indicate initial retreat in this trough was underway by 21.5–21.6 cal ka BP. This is consistent with surface exposure dates from ice-moulded bedrock surfaces and erratic boulders which show that initial onshore thinning of NEGIS during deglaciation commenced at 22.9–22.5 ka BP (Roberts et al., 2024). A subsequent date on deglacial glacial marine sediments from further inshore in the trough indicates the grounding line had cleared the outer shelf by 18.6 cal ka BP (Fig. 8). Hence, retreat of ice from the shelf-edge and outer shelf in both Norske and Westwind troughs took place during the last glaciation. This directly supports an extensive GrIS at the LGM in the cross-shelf bathymetric troughs offshore of northeast Greenland. Such early retreat of the northeast sector of the ice sheet contrasts with some other sectors, notably central west Greenland bordering Baffin Bay where shelf-edge retreat commenced several thousand years later at 16–17 cal ka BP (e.g., Jennings et al., 2017).

Rasmussen et al. (2022) present a palaeoceanographic study of a core collected from the shelf-edge at 79.4°N, south of the mouth of Westwind Trough. The lower part of the core comprises a diamict, interpreted as an iceberg turbate, with dates which span the LGM. Based on these data Rasmussen et al. (2022) argue that the GrIS did not reach the shelf-edge in this location during the LGM. Arndt et al. (2017) also argued on the basis of geomorphological and acoustic data that the LGM GrIS did not ground to the shelf-edge between Norske and Westwind troughs on the basis of extensive zones of iceberg ploughed terrain at the shelf-edge across the banks, although their study lacked dating control. Collectively, therefore, the new findings from our study, combined with this previous work, indicate that the ice-sheet configuration at the LGM was one in which fast-flowing ice was grounded to the shelf-edge in both Westwind and Norske troughs but ice may have been more restricted on at least parts of the intervening shallow banks. Palaeo-glaciologically therefore the grounded ice in both troughs may have been in the form of fast-flowing outlets, at least on the outer shelf, rather than ice streams sensu-stricto that were bordered by slower moving ice along the length of the troughs.

Initial retreat from the shelf-edge and subsequent recession across the outer shelf took place during Greenland Stadial 2.1 (22.9–17.4 ka BP). Atmospheric warming is therefore unlikely as a trigger for initial

deglaciation from the shelf-edge. Rasmussen et al. (2022) presented microfossil evidence for strong flow of relatively warm subsurface Atlantic Water at the shelf-edge south of Westwind Trough between 25 and c. 17.5 ka. Devendra et al. (2022) also report a small increase in Atlantic Water advection on to the shelf between 18.5 and 16.5 ka. Hence, ocean warming is a more likely potential trigger for initial GrIS retreat in both troughs.

Our radiocarbon dates imply that the timing of retreat may have been asynchronous between the two troughs, with retreat underway by 21.6 ka in Norske Trough but not until ≥ 19 ka in Westwind Trough. This implies that adjacent fast flowing outlets during the LGM on the northeast Greenland margin responded asynchronously to external forcing; an interpretation that is consistent with observations elsewhere in Greenland on the retreat of large marine-terminating outlet glaciers on the continental shelf following the LGM (e.g., Jennings et al., 2017). The asynchronous retreat may also be linked to variability in ocean forcing potentially driving initial retreat. While both Westwind and Norske troughs receive Atlantic sourced water at the present day, the Atlantic water in Westwind Trough (Arctic Atlantic Water) is cooler than the Atlantic Intermediate Water seen in Norske Trough (Schaffer et al., 2017, 2020). If such a difference persisted during glacial times it might explain the earlier retreat in Norske Trough in comparison to Westwind Trough.

Grounding-line retreat across the shelf took place in a glacial marine environment in which the ice sheet appears to have terminated as a floating ice shelf rather than a grounded tidewater margin, although it is possible that the latter occurred in Westwind Trough. Retreat rates of grounded ice during this early phase of retreat were 23 m a⁻¹ and 19 m a⁻¹ for retreat in Norske and Westwind troughs, respectively. These are an order of magnitude slower compared with outer shelf retreat rates of other Greenland palaeo-ice streams such as Ummannaq and Jakobshavn Isbrae (Roberts et al., 2013; Ó Cofaigh et al., 2013a), and although outer Norske Trough has a reverse bed-slope gradient it appears that bathymetry did not exert a strong control on early retreat rates of the ancestral NEGIS. Based on radiocarbon dated cores from inner Norske Trough retreat rates then increase from the mid/outer to inner trough (Fig. 8). From the outer trough site of PS100-144 retreat rates increase to approximately 32 m a⁻¹ to core DA17/92G (Davies et al., 2022), then 40 m a⁻¹ through to PS100-198 and to 60 m a⁻¹ into the embayment in front of the current ice shelf, core PS100-270 (Fig. 8) (Lloyd et al., 2023). Lloyd et al. (2023) suggested this increased rate in retreat through the inner shelf may be linked to warming of the ocean waters through to the early Holocene.

6. Conclusions

Geomorphological, sedimentological and chronological data from two large cross-shelf bathymetric troughs are used to reconstruct the LGM history of the GrIS on the continental shelf offshore of northeast Greenland.

- Landform and sedimentary evidence in the form of streamlined subglacial lineations, grounding-zone wedges, subglacial till and ice proximal grounding-line sediments indicate that the GrIS was grounded to the shelf-edge in Westwind and Norske troughs.
- Radiocarbon dates from this study provide the first direct chronological constraints on the age of the most recent phase of shelf-edge glaciation offshore of northeast Greenland. Dates on deglacial sediments on the outer shelf indicate a LGM age for this most recent shelf-edge advance in both troughs.
- Initial retreat of the GrIS from the shelf-edge took place at c. 21.6–21.5 ka BP in Norske Trough and 19 ka BP in Westwind Trough. This indicates that adjacent marine-terminating outlets of the GrIS responded asynchronously to external forcing during the last deglaciation of the northeast Greenland continental shelf.

- Grounding-line retreat rates across the outer shelf during the last deglaciation were slow (19–23 m a⁻¹) in both Westwind and Norske troughs. In Norske Trough retreat rates then gradually increase (32–60 m a⁻¹) through to the inner-most shelf from c. 15 to 9 ka BP.
- Palaeo-glaciologically the LGM configuration of the GrIS on the continental shelf offshore of northeast Greenland was one of fast flowing outlets which extended to the shelf-edge but across the intervening shallower banks the ice sheet extent may have been more restricted.

Author contributions

Colm Ó Cofaigh: Writing original draft, writing review & editing, Conceptualisation, Investigation (cruise participation), Interpretation, Funding acquisition., Jeremy M. Lloyd: Writing review & editing, Conceptualisation, Investigation (Cruise Participation), Interpretation, Funding acquisition; S. Louise Callard: Writing review & editing, Investigation (Cruise Participation); Catalina Gebhardt: Writing review & editing, data processing and figure preparation; Katharina T. Streuff: Writing review & editing, Investigation (Cruise Participation); Boris Dorschel Writing review & editing; James A. Smith: review and interpretation; Timothy P. Lane, Review and interpretation, figure preparation; Stewart S.R. Jamieson, Review and interpretation, figure preparation; Torsten Kanzow: writing review & editing, investigation (cruise participation); David H. Roberts Writing review and editing, Conceptualisation (project lead), Interpretation, Funding acquisition.

Declaration of competing interest

The authors declare that they have no known competing financial interests or personal relationships that could have appeared to influence the work reported in this paper.

Acknowledgements

This work was funded by the UK Natural Environment Research Council (NERC) grant NE/N011228/1 and radiocarbon grant 2113.0418. We thank the Officers and crews of the RV Polarstern during cruises PS100 and PS109 for their excellent support. We gratefully acknowledge support from the Alfred Wegener Institute (AWI) for ship time via grants AWI_PS100_01 and AWI_PS109_03. We thank Chris Orton in the Design and Imaging Unit (Geography) at Durham University for assistance with figures. We thank the reviewers Renata Lucchi, Andrew Newton and an anonymous reviewer for their comments on the original manuscript and the handling editor Dr. Antje Voelker for her assistance during the revision process.

Data availability

Data are available from the PANGAEA data centre (Alfred Wegener Institute, Helmholtz Center for Polar and Marine Research, Germany) and the UK NERC Polar Data Centre (<http://www.bas.ac.uk/data/uk-pdc/>).

References

Alfred-Wegener-Institut Helmholtz-Zentrum für Polar- und Meeresforschung, 2017. Polar Research and supply vessel POLARSTERN operated by the Alfred-Wegener-Institute. *Journal of large-scale research facilities* 3, A119. <https://doi.org/10.17815/jlsrf-3-163>.

An, L., Rignot, E., Wood, M., Willis, J.K., Mougnot, J., Khan, S.A., 2021. Ocean melting of the Zachariae Isstrøm and Nioghalvfjærdssjorden glaciers, northeast Greenland. *Proceedings of the National Academy of Science* 118, e2015483118. <https://doi.org/10.1073/pnas.2015483118>.

Arndt, J.E., 2015. Marine geomorphological record of ice sheet development in east Greenland since the last glacial maximum. *J. Quat. Sci.* 33, 853–864.

Arndt, J.E., Jokat, W., Dorschel, B., Myklebust, R., Dowdeswell, J.A., Evans, J., 2015. A new bathymetry of the Northeast Greenland continental shelf: constraints on glacial and other processes. *G-cubed* 16, 3733–3753. <https://doi.org/10.1002/2015GC005931>.

Arndt, J.E., Jokat, W., Dorschel, B., 2017. The last glaciation and deglaciation of the Northeast Greenland continental shelf revealed by hydro-acoustic data. *Quat. Sci. Rev.* 160, 45–56. <https://doi.org/10.1016/j.quascirev.2017.01.018>.

Aschwanden, A., Fahnestock, M.A., Truffer, M., Brinkerhoff, D.J., Hock, R., Khroulev, C., Mottram, R., Khan, S.A., 2019. Contribution of the Greenland Ice Sheet to sea level over the next millennium. *Sci. Adv.* 5 (6), eaav9396.

Barnes, P.W., Lien, R., 1988. Icebergs rework shelf sediments to 500 m off Antarctica. *Geology* 16 (12), 1130–1133.

Batchelor, C.L., Dowdeswell, J.A., 2015. Ice-sheet grounding-zone wedges (GZWs) on high-latitude continental margins. *Mar. Geol.* 363, 65–92.

Bennike, O., Björck, S., 2002. Chronology of the last recession of the Greenland ice sheet. *J. Quat. Sci.* 17, 211–219. <https://doi.org/10.1002/jqs.670>.

Bradwell, T., Small, D.P., Fabel, D., Smedley, R.K., Clark, C.D., Saher, M., Callard, S.L., Chiverell, R.C., Dove, D., Moreton, S.G., Roberts, D.H., Dueller, G.A.T., Ó Cofaigh, C., 2019. Ice-stream demise dynamically conditioned by trough shape and bed strength. *Sci. Adv.* 5 (4) article No. eaau1380.

Briner, J.P., Stewart, H.A.M., Young, N.E., Phillips, W., Losee, S., 2010. Using proglacial-threshold lakes to constrain fluctuations of the Jakobshavn Isbrae ice margin, western Greenland, during the Holocene. *Quat. Sci. Rev.* 29, 3861–3874.

Callard, S.L., Ó Cofaigh, C., Benetti, S., Chiverrell, R.C., van Landeghem, K., Saher, M., Gales, J., Small, D., Clark, C.D., Livingstone, S.J., Fabel, D., 2018. Extent and retreat history of the Barra Fan Ice Stream offshore western Scotland and northern Ireland during the last glaciation. *Quat. Sci. Rev.* 201, 280–302.

Callard, S.L., Ó Cofaigh, C., Lloyd, J.M., Smith, J.A., Gebhardt, C., Kanzow, T., Roberts, D. H. (submitted). Ocean driven retreat of the Northeast Greenland ice stream following the last glacial maximum. *Nat. Comms.*

Davies, J., Möller Mathiasen, A., Kristiansen, K., Hansen, K.E., Wacker, L., Olsen Alstrup, A.K., Munk, A.L., Pearce, C., Seidenkrantz, M.-S., 2022. Linkages between ocean circulation and the Northeast Greenland ice stream in the early Holocene. *Quat. Sci. Rev.* 286, 107530. <https://doi.org/10.1016/j.quascirev.2022.107530>.

Devendra, D., Łącka, M., Telesinski, M.M., Rasmussen, T.L., Szybor, K., Zajaczkowski, M., 2022. Paleooceanography of the northwestern Greenland sea and return Atlantic current evolution, 35–4 kyr BP. *Global Planet. Change* 217, 103947.

Domack, E., Jacobson, E., Shipp, S., Anderson, J., 1999. Late Pleistocene-Holocene retreat of the West Antarctic ice-sheet system in the Ross Sea: Part 2 - sedimentologic and stratigraphic signature. *Geol. Soc. Am. Bull.* 111, 1517–1536.

Dowdeswell, J.A., Ó Cofaigh, C., Pudsey, C.J., 2004. Thickness and extent of the subglacial till layer beneath an Antarctic paleo-ice stream. *Geology* 32, 13–16.

Dowdeswell, J.A., Fugelli, E.M.G., 2012. The seismic architecture and geometry of grounding-zone wedges formed at the marine margins of past ice sheets. *Geol. Soc. Am. Bull.* 124, 1750–1761.

Dowdeswell, J.A., Whittington, R.J., Marienfeld, P., 1994. The origin of massive diamicton facies by iceberg rafting and scouring, Scoresby Sund, East Greenland. *Sedimentology* 41, 21–35.

Elverhøi, A., Norem, H., Andersen, E.S., Dowdeswell, J.A., Fossen, I., Hafliðason, H., Kenyon, N.H., Laberg, J.S., King, E.L., Sejrup, H.P., Solheim, A., Vorren, T.O., 1997. On the origin and flow behaviour of submarine slides on deep sea fans along the Norwegian-Barents Sea continental margin. *Geo Mar. Lett.* 17, 119–125.

Evans, D.J.A., 2018. *Till: A Glacial Process Sedimentology*. Wiley-Blackwell, Chichester.

Evans, J., Ó Cofaigh, C., Dowdeswell, J.A., Wadhams, P., 2009. Marine geophysical evidence for former expansion and flow of the Greenland Ice Sheet across the northeast Greenland continental shelf. *J. Quat. Sci.* 24, 279–293. <https://doi.org/10.1002/jqs.1231>.

Evans, J., Pudsey, C.J., Ó Cofaigh, C., Morris, P., Domack, E., 2005. Late Quaternary glacial history, flow dynamics and sedimentation along the eastern margin of the Antarctic Peninsula Ice Sheet. *Quaternary Science Reviews* 24, 741–774.

Eyles, C.H., Eyles, N., 2000. Subaqueous mass-flow origin for lower perian diamictites and associated facies of the grant group, barbwire terrace, canning basin, western Australia. *Sedimentology* 47, 343–356.

Graham, A.G.C., Larter, R.D., Gohl, K., Hillenbrand, C.-D., Smith, J.A., Kuhn, G., 2009. Bedform signature of a West Antarctic palaeo-ice stream reveals a multi-temporal record of flow and substrate control. *Quat. Sci. Rev.* 28, 2774–2793.

Hansen, K.E., Lorenzen, J., Davies, J., Wacker, L., Pearce, C., Seidenkrantz, M.-S., 2022. Deglacial to mid-Holocene environmental conditions on the northeastern Greenland shelf, western Fram Strait. *Quat. Sci. Rev.* 293, 107704.

Heaton, T.J., Butzin, M., Bard, E., Bronk Ramsey, C., Hughen, K.A., Köhler, P., Reimer, P. J., 2023. Marine radiocarbon calibration in polar regions: a simple approximate approach using Marine20. *Radiocarbon* 65 (4), 848–875. <https://doi.org/10.1017/RDC.2023.42>.

Heaton, T.J., Vohler, P., Butzin, M., Bard, E., Reimer, R.W., Austin, W.E.N., Bronk Ramsey, C., Grootes, P.M., Hughen, K.A., Kromer, B., Reimer, P.J., Adkins, J., Burke, A., Cook, M.S., Olsen, J., Skinner, L.C., 2020. Marine20 - the marine radiocarbon age calibration curve (0–55,000 cal BP). *Radiocarbon* 62, 779–820.

Hogan, K., Ó Cofaigh, C., Jennings, A.E., Dowdeswell, J.A., Hiemstra, J.F., 2016. Deglaciation of a major palaeo-ice stream in disko trough, west Greenland. *Quat. Sci. Rev.* 147, 5–26.

Jennings, A.E., Andrews, J.T., Ó Cofaigh, C., Onge, St, Sheldon, C. Belt, Cabedo-Sanz, Hillaire-Marcel, C.M., 2017. Ocean forcing of ice sheet retreat in Central West Greenland from LGM through deglaciation. *Earth Planet Sci. Lett.* 472, 1–13.

Jennings, A.E., Andrews, J.T., Ó Cofaigh, C., St-Onge, G., Belt, S., Cabedo-Sanz, P., Pearce, C., Hillaire-Marcel, C., D. Calvin Campbell, D.C., 2018. Baffin Bay

- paleoenvironments in the LGM and HS1: resolving the ice-shelf question. *Mar. Geol.* 402, 5–16.
- Jennings, A.E., Reilly, B., Andrews, J., Hogan, K., Walczak, M., Jakobsson, M., Stoner, J., Mix, A., Nicholls, K., O'Regan, M., Prins, M., Troelstra, S., 2022. Modern and early Holocene ice shelf sediment facies from Petermann Fjord and northern Nares Strait, northwest Greenland. *Quat. Sci. Rev.* 283. <https://doi.org/10.1016/j.quascirev.2022.107460>.
- Khan, S.A., Kjær, K.H., Bevis, M., Bamber, J.L., Wahr, J., Kjeldsen, K.K., Bjørk, A.A., Korsgaard, N.J., Stearns, L.A., van den Broeke, M.R., Liu, L., Larsen, N.K., Muresan, I. S., 2014. Sustained mass loss of the northeast Greenland ice sheet triggered by regional warming. *Nat. Clim. Change* 4, 292–299. <https://doi.org/10.1038/nclimate2161>.
- Khan, S.A., Choi, Y., Morlighem, M., Rignot, E., Helm, V., Humbert, A., Mouginit, J., Millan, R., Kjær, K.H., Bjørk, A.A., 2022. Extensive inland thinning and speed-up of northeast Greenland ice stream. *Nature* 611, 727–732.
- Kilfeather, A.A., Ó Cofaigh, C., Lloyd, J.M., Dowdeswell, J.A., Xu, S., Moreton, S., 2011. Ice stream retreat and ice shelf history in Marguerite Bay, Antarctic Peninsula: sedimentological and foraminiferal signatures. *Geol. Soc. Am. Bull.* 123, 997–1015.
- Kilfeather, A.A., Ó Cofaigh, C., Dowdeswell, J.A., van der Meer, J., Evans, D.J.A., 2010. Micromorphological characteristics of glacial marine sediments. *Geo Mar. Lett.* 30, 77–97.
- Laberg, J.S., Vorren, T.O., 1995. Late weichselian submarine debris flow deposits on the bear Island trough mouth fan. *Mar. Geol.* 127, 45–72.
- Laberg, J.S., Vorren, T.O., 2000. Flow behaviour of the submarine glacial debris flows on the bear Island trough mouth fan, western barents sea. *Sedimentology* 47, 1105–1117.
- Laberg, J.S., Forwick, M., Husum, K., 2017. New geophysical evidence for a revised maximum position of part of the NE sector of the Greenland ice sheet during the last glacial maximum. *Arktos* 3, 3. <https://doi.org/10.1007/s41063-017-0029-4>.
- Lane, T.P., Roberts, D.H., Ó Cofaigh, C., Vieli, A., Moreton, S.G., 2015. The glacial history of the southern Svartenhuk Halvø, West Greenland. *Arktos* 1, 1–28.
- Lane, T.P., Darvill, C., Rea, B.R., Bentley, M.J., Smith, J.A., Jamieson, S.R., Ó Cofaigh, C., Roberts, D.H., 2023. The geomorphological record of an ice stream to ice shelf transition in Northeast Greenland. *Earth Surf. Process. Landf.* 48, 1321–1341.
- Larsen, N.K., Levy, L.B., Carlson, A.E., Buizert, C., Olsen, J., Strunk, A., Bjørk, A.A., Skov, D.S., 2018. Instability of the Northeast Greenland ice stream over the last 45,000 years. *Nat. Commun.* 9, 1872. <https://doi.org/10.1038/s41467-018-04312-7>.
- Li, G., Piper, D.W., Campbell, D.C., 2011. The quaternary lancaster sound trough-mouth fan, NW Baffin Bay. *J. Quat. Sci.* 26, 511–522.
- Lindeman, M.R., Straneo, F., Wilson, N.J., Toole, J.M., Krishfield, R.A., Beaird, N.L., 2020. Ocean circulation and variability beneath Nioghalvfjærdsbræ (79 North Glacier) ice tongue. *J. Geophys. Res.: Oceans* 125, e2020JC016091. <https://doi.org/10.1029/2020JC016091>.
- Lloyd, J.M., Park, L.A., Kuijpers, A., Moros, M., 2005. Early Holocene palaeoceanography and deglacial chronology of Disko Bugt, west Greenland. *Quat. Sci. Rev.* 24, 1741–1755.
- Lloyd, J.M., Ribeiro, S., Weckström, K., Callard, L., Ó Cofaigh, C., Leng, M.J., Gulliver, P., Roberts, D.H., 2023. Ice-ocean interactions at the Northeast Greenland Ice stream (NEGIS) over the past 11,000 years. *Quat. Sci. Rev.* 308, 108068.
- López-Quiros, A., Junna, T., Davies, J., Andresen, K., Nielsen, T., Haghypour, N., Wacker, L., Alstrup, A.K., Munk, O.L., Rasmussen, T.L., Pearce, C., Marit-Solveig Seidenkrantz, M.S., 2024. Retreat patterns and dynamics of the former Norske Trough ice stream (NE Greenland): an integrated geomorphological and sedimentological approach. *Quat. Sci. Rev.* 325, 108477.
- Lucchi, R.G., Camerlenghi, A., Rebecco, M., et al., 2013. Postglacial sedimentary processes on the Storfjorden and Kveithola trough mouth fans: significance of extreme glacial marine sedimentation. *Global Planet. Change* 111, 309–326.
- Mackiewicz, N., Powell, R., Carlson, P., Molnia, B., 1984. Interlaminated ice-proximal glacial marine sediments in Muir Inlet, Alaska. *Mar. Geol.* 57, 113–147.
- Mayer, C., Schaffer, J., Hattermann, T., Floricioiu, D., Krieger, L., Dodd, P.A., Kanzow, T., Licciulli, C., Schannwell, C., 2018. Large ice loss variability at Nioghalvfjærdsfjorden Glacier, northeast-Greenland. *Nat. Commun.* 9, 2768. <https://doi.org/10.1038/s41467-018-05180-x>.
- Mouginit, J., Rignot, E., Scheuchl, B., Fenty, I., Khazendar, A., Morlighem, M., Buzzi, A., Paden, J., 2015. Fast retreat of Zacharie Isstrøm, northeast Greenland. *Science* 350, 1357–1361. <https://doi.org/10.1126/science.aac7111>.
- Mulder, T., Alexander, J., 2001. The physical character of subaqueous sedimentary density flows and their deposits. *Sedimentology* 48, 269–299.
- Newton, A.M.W., Knutz, P.C., Huuse, M., Gannon, P., Brocklehurst, S.H., Clausen, O.R., Gong, Y., 2017. Ice stream reorganization and glacial retreat on the northwest Greenland shelf. *Geophys. Res. Lett.* 44, 7826–7835.
- Ó Cofaigh, C., Dowdeswell, J.A., 2001. Laminated sediments in glacial marine environments: diagnostic criteria for their interpretation. *Quat. Sci. Rev.* 20, 1411–1436. [https://doi.org/10.1016/S0277-3791\(00\)00177-3](https://doi.org/10.1016/S0277-3791(00)00177-3).
- Ó Cofaigh, C., Pudsey, C.J., Dowdeswell, J.A., Morris, P., 2002. Evolution of subglacial bedforms along a paleo-ice stream, Antarctic Peninsula continental shelf. *Geophys. Res. Lett.* 29 (8). <https://doi.org/10.1029/2001GL014488>.
- Ó Cofaigh, C., Dowdeswell, J.A., Evans, J., Kenyon, N.H., Taylor, J., Mienert, J., Wilken, M., 2004. Timing and significance of glacially-influenced mass-wasting in the submarine channels of the Greenland Basin. *Mar. Geol.* 207, 39–54.
- Ó Cofaigh, C., Larter, R.D., Dowdeswell, J.A., Hillenbrand, C.-D., Pudsey, C.J., Evans, J., Morris, P., 2005. Flow of the west Antarctic ice sheet on the continental margin of the Bellingshausen sea at the last glacial maximum. *J. Geophys. Res.* 110. <https://doi.org/10.1029/2005JB003619>.
- Ó Cofaigh, C., Evans, J., Dowdeswell, J.A., Larter, R.D., 2007. Till characteristics, genesis and transport beneath Antarctic paleo-ice streams. *J. Geophys. Res.* 112, F03006, 101029/2006JF000606.
- Ó Cofaigh, C., Dowdeswell, J.A., Jennings, A.E., Hogan, K., Kilfeather, A., Hiemstra, J.F., Noormets, R., Evans, J., McCarthy, D.J., Andrews, J.T., Lloyd, J.M., Moros, M., 2013a. An extensive and dynamic ice sheet on the West Greenland shelf during the last glacial cycle. *Geology* 41, 219–222.
- Ó Cofaigh, C., Andrews, J.T., Jennings, A.E., Dowdeswell, J.A., Kilfeather, A.A., Hogan, K., Sheldon, C., 2013b. Glacial marine lithofacies, provenance, and depositional processes on a West Greenland trough-mouth fan. *J. Quat. Sci.* 28, 13–26.
- Ó Cofaigh, C., Hogan, K.A., Jennings, A.E., Callard, S.L., Dowdeswell, J.A., Noormets, R., Evans, J., 2018. The role of meltwater in high-latitude trough-mouth fan development: the Disko Trough-Mouth Fan, West Greenland. *Mar. Geol.* 402, 17–32.
- Ó Cofaigh, C., Callard, S.L., Roberts, D.H., Chiverrell, R.C., Ballantyne, C.K., Evans, D.J.A., Saher, M., Van Landeghem, K., Smedley, R., Benetti, S., Burke, M.J., Clark, C.D., Duller, G.A.T., Fabel, D., Livingstone, S.J., McCarron, S., Medialdea, A., Moreton, S., Sacchetti, F., 2021. Timing and pace of ice-sheet withdrawal across the marine-terrestrial transition west of Ireland during the last glaciation. *J. Quat. Sci.* 36, 805–832.
- Olsen, I.L., Rydningen, T.A., Forwick, M., Laberg, J.S., Husum, K., 2020. Last glacial ice sheet dynamics offshore NE Greenland – a case study from store Koldewey trough. *Cryosphere* 14, 4475–4494.
- Ottesen, D., Dowdeswell, J.A., 2009. An inter-ice-stream glaciated margin: submarine landforms and a geomorphic model based on marine-geophysical data from Svalbard. *Geol. Soc. Am. Bull.* 121, 1647–1665.
- Powell, R.D., Domack, E.W., 1995. Modern glaciomarine environments. In: Menzies, J. (Ed.), *Glacial Environments*, vol. 1. Butterworth-Heinemann, Oxford, pp. 445–486. *Modern Glacial Environments: Processes, Dynamics and Sediments*.
- Pudsey, C.J., Evans, J., 2001. First survey of Antarctic sub-ice shelf sediments reveals mid-Holocene ice shelf retreat. *Geology* 29, 787–790.
- Rasmussen, T.L., Pearce, C., Andresen, K.J., Nielsen, T., Seidenkrantz, M.S., 2022. Northeast Greenland: ice-free shelf edge at 79.4° N around the Last Glacial Maximum 25.5–17.5 ka. *Boreas* 51, 759–775.
- Reimer, P.J., Reimer, R.W., 2001. A marine reservoir correction database and on-line interface. *Radiocarbon* 43 (2A), 461–463. <https://doi.org/10.1017/S0033822200038339>.
- Rignot, E.J., Kanagaratnam, P., 2006. Changes in the velocity structure of the Greenland ice sheet. *Science* 311, 986–990. <https://doi.org/10.1126/science.1121381>.
- Rignot, E., Xu, Y., Menemenlis, D., Mouginit, J., Scheuchl, B., Li, X., Morlighem, M., Seroussi, H., van den Broeke, M., Fenty, I., Cai, C., An, L., de Fleurian, B., 2016. Modeling of ocean-induced ice melt rates of five west Greenland glaciers over the past two decades. *Geophys. Res. Lett.* 43, 6374–6382.
- Roberts, D.H., Rea, B.R., Lane, T.P., Schnabel, C., Rodés, A., 2013. New constraints on Greenland ice sheet dynamics during the last glacial cycle: evidence from the Ummannaq ice stream system. *Journal of Geophysical Research - Earth Surface* 118, 519–541.
- Roberts, D.H., Lane, T.P., Jones, R.S., Bentley, M.J., Darvill, C.M., Rodes, A., Smith, J.A., Jamieson, S.S., Rea, B.R., Fabel, D., Gheorghiu, D., 2024. The deglacial history of 79N glacier and the Northeast Greenland Ice Stream. *Quat. Sci. Rev.* 336, 108770.
- Schaffer, J., Kanzow, T., von Appen, W.-J., von Albedyll, L., Arndt, J.E., Roberts, D.H., 2020. Bathymetry constrains ocean heat supply to Greenland's largest glacier tongue. *Nat. Geosci.* 13, 227–231.
- Schaffer, J., Appen, W.-J., von, Dodd, P.A., Hofstede, C., Mayer, C., Steur, L. de, Kanzow, T., 2017. Warm water pathways toward Nioghalvfjærdsfjorden Glacier, northeast Greenland. *J. Geophys. Res.: Oceans* 122, 4004e4020. <https://doi.org/10.1002/2016JC012462>.
- Skov, D.S., Andersen, J.L., Olsen, J., Jacobsen, B.H., Knudsen, M.F., Jansen, J.D., Larsen, N.K., Egholm, D.L., 2020. Constraints from cosmogenic nuclides on the glaciation and erosion history of Dove Bugt, northeast Greenland. *Geol. Soc. Am. Bull.* 132, 2282–2294.
- Slabon, P., Dorschel, B., Jokat, W., Myklebust, R., Hebbeln, D., Gebhardt, C., 2016. Greenland ice sheet retreat history in the northeast Baffin Bay based on high-resolution bathymetry. *Quat. Sci. Rev.* 154, 182–198.
- Smith, J.A., Graham, A.G.C., Post, A.L., Hillenbrand, C.D., Bart, P.J., Powell, R.D., 2019. The marine geological imprint of Antarctic ice shelves. *Nat. Commun.* 10, 5635.
- Straneo, F., Heimbach, P., 2013. North Atlantic warming and the retreat of Greenland's outlet glaciers. *Nature* 504, 36–43. <https://doi.org/10.1038/nature12854>.
- Straneo, F., Sutherland, D.A., Stearns, L.A., Catania, G.A., Catania, G., Heimbach, P., et al., 2019. The case for a sustained Greenland ice sheet-ocean observing system (GrIOOS). *Front. Earth Sci.* 6 (138), 391. <https://doi.org/10.3389/feart.2019.00138>.
- Streuff, K., Ó Cofaigh, C., Hogan, K.A., Jennings, A.E., Lloyd, J., Noormets, R., Nielsen, T., Kuijpers, A., Dowdeswell, J.A., Weinrebe, W., 2017. Seafloor geomorphology and glacial marine sedimentation associated with fast-flowing ice sheet outlet glaciers in Disko Bay, West Greenland. *Quat. Sci. Rev.* 169, 206–230.
- Stuiver, M., Reimer, P.J., 1993. Radiocarbon 35, 215–230. *Calib* 8.20. <http://calib.org/calib/>.
- Syring, N., Lloyd, J.M., Stein, R., Fahl, K., Roberts, D.H., Callard, L., Ó Cofaigh, C., 2020. Holocene interactions between glacier retreat, sea ice formation, and Atlantic water advection at the inner Northeast Greenland continental shelf. *Paleoceanogr. Paleoclimatol.* 35, e2020PA004019. <https://doi.org/10.1029/2020PA004019>.
- Talling, P.J., Masson, D.G., Sumner, E.J., Melgesini, G., 2012. Subaqueous sediment density flows: depositional processes and deposit types. *Sedimentology* 59, 1937–2003.

- von Albedyll, L., Schaffer, J., Kanzow, T., 2021. Ocean variability at Greenland's largest glacier tongue linked to continental shelf circulation. *J. Geophys. Res.: Oceans* 126, e2020JC017080.
- Vorren, T.O., Hald, M., Edvardsen, M., Ow, L.H., 1983. *Glacigenic Sediments and Sedimentary Environments on Continental Shelves: General Principles with a Case Study from the Norwegian Shelf*.
- Walker, M., 2005. *Quaternary Dating Methods*. Wiley, pp. 304–pp.
- Wekerle, C., McPherson, R., von Appen, W.-J., Wang, Q., Timmermann, R., Scholz, P., Danilov, S., Shu, Q., Kanzow, T., 2024. Atlantic Water warming increases melt below Northeast Greenland's last floating ice tongue. *Nat. Commun.* <https://doi.org/10.1038/s41467-024-45650-z>.
- Wilson, N.J., Straneo, F., 2015. Water exchange between the continental shelf and the cavity beneath nioghalvfjærdsbræ (79 north glacier). *Geophysical Research Letters* 42, 7648–7654.
- Winkelmann, D., Jokat, W., Jensen, L., Schenke, H.-W., 2010. Submarine end moraines on the continental shelf off NE Greenland: implications for Lateglacial dynamics. *Quat. Sci. Rev.* 29, 1069–1077. <https://doi.org/10.1016/j.quascirev.2010.02.002>.
- Young, N.E., Briner, J.P., Axford, Y., Csatho, B., Babonis, G.S., Rood, D.H., Finkel, R.C., 2011. Response of a marine-terminating Greenland outlet glacier to abrupt cooling 8200 and 9300 years ago. *Geophys. Res. Lett.* 38, L24701.